THE SWAT TEAM

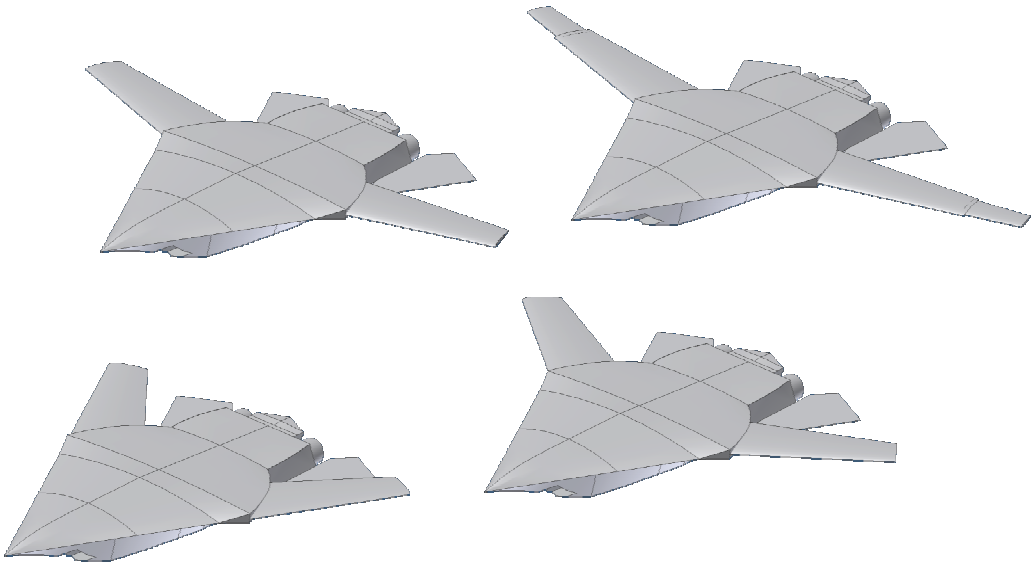

2002/2003 AE DESIGN
SPRING FINAL REPORT
MAY 1, 2003

THE SWAT TEAM

SMART WING ADAPTIVE TECHNOLOGIES

May 1, 2002

Team Roster:

Team Member	**Signature**
David Hall	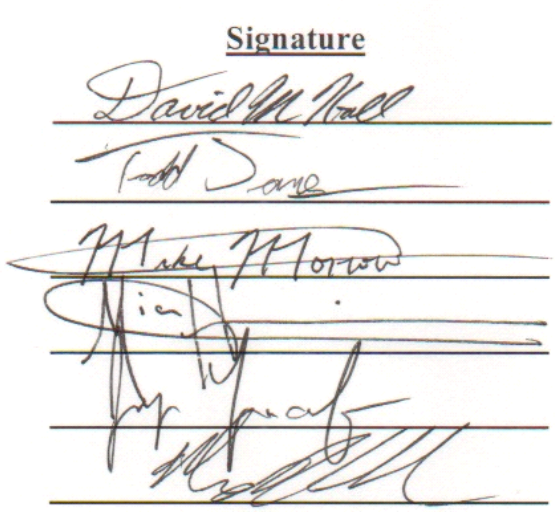
Todd Jones	
Mike Morrow	
Mian Hussain	
Yoseph Yacob	
Matt Allen	

Faculty Advisor:

Dr. William H. Mason

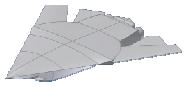

1 EXECUTIVE SUMMARY

The SWAT Team aircraft design team was created in August 2002 in response to a request for proposal put forth by the Virginia Tech Aerospace Engineering Department in conjunction with the United States Air Force. This request for proposal calls for the development of an aircraft to be used as a technology demonstrator for morphing technology. Additionally, the request for proposal requires the classification of morphing methods and missions in which these technologies would be beneficial.

After consideration of several mission types it was determined that a military application would benefit the most from morphing technologies and provide a better platform for a demonstration aircraft. A multi-mission Fighter/Attack profile was selected, with four different mission profiles under this general topic being selected for detailed mission analysis. The four missions selected were: Combat Air Patrol, Medium Range Strike, Close Air Support, and Recon-Quick Strike. These missions were selected because they represent the wide range of missions a truly multi-mission capable aircraft would be expected to perform. Though several aircraft are currently capable of accomplishing several of the mission profiles, current aircraft are all optimized for one specific mission. A morphing aircraft would be able to optimize itself for every mission.

Several initial concepts were investigated, each using a different combination of morphing technologies. Two concepts, a variable sweep concept and a telescoping wing concept were selected for further performance analysis and comparison. The results of this analysis led to the blending of the two technologies into a third and final concept which created an aircraft, seen in Figure 1.1 and designated the SWAT-5 Mako, with better all around performance.

This final concept utilizes variable sweep and telescoping wing technologies for its mission morphing capabilities. For control morphing the concept utilizes variable camber, smart controls, and adaptive torque control technologies. The SWAT-5 is 45’ in length with a span ranging from

40’ to 76’ and a maximum Take-Off Gross Weight of approximately 37,000 lbs. When compared with a fixed wing control aircraft, the Mako is capable of achieving a 27% reduction in landing distance, a 29% reduction in takeoff distance, 32% increase in range, and 21% increase in endurance time through the use of its morphing surfaces, as seen in Table 1.1.

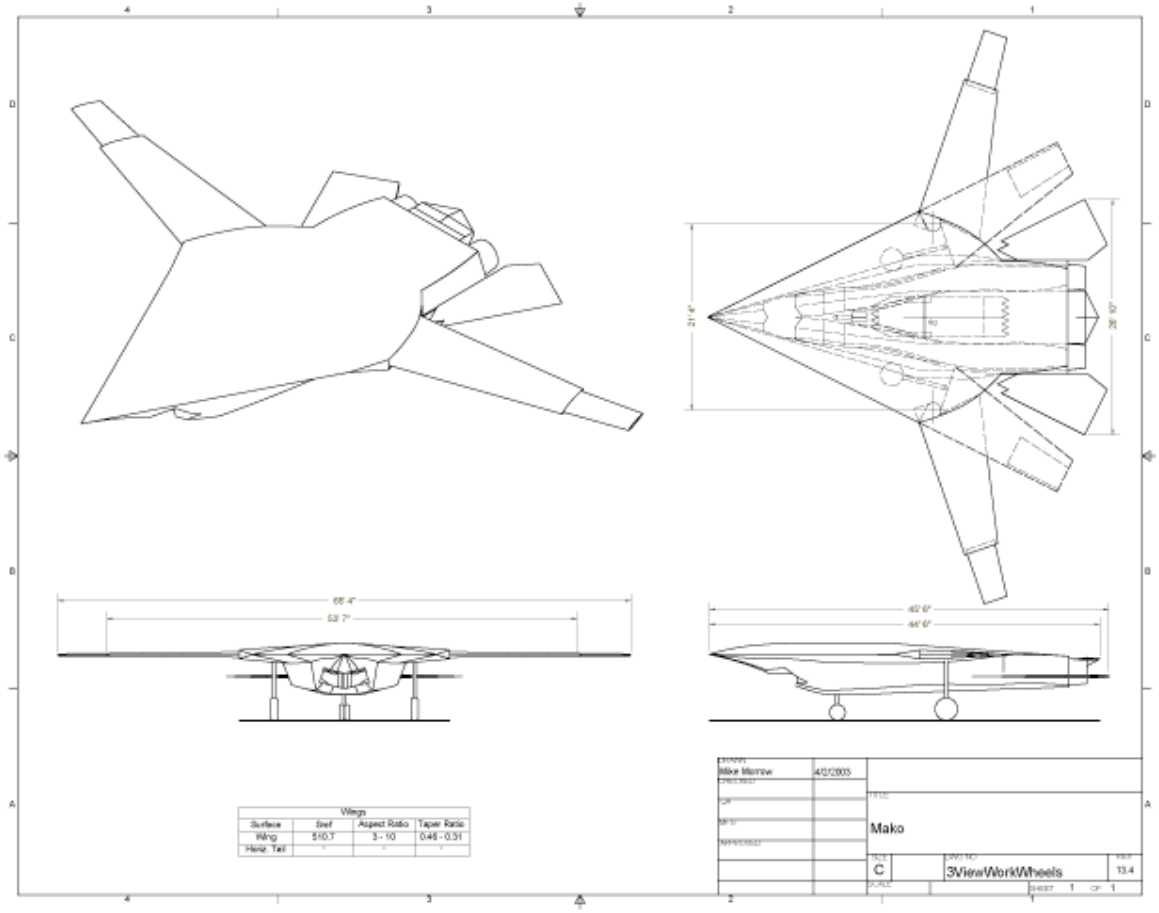

Figure 1.1: The SWAT-5 Mako

Table 1.1: Morphing benefits

Configuration	*Cl*	*Max Rate of Climb (ft/s)*	*Takeoff Distance (ft)*	*Landing Distance (ft)*	*Range (nm)*	*Endurance (hours)*
SWAT-5 Morphing	0.48	48,657	1,776	4,261	4,190	7.75
SWAT-5 40 degrees	0.45	47,317	2,489	5,817	3,157	6.41
Benefit	7%	3%	29%	27%	33%	21%

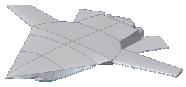

2 TABLE OF CONTENTS

3 INDEXES

3.1 Index of Tables

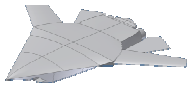

3.2 Index of Figures

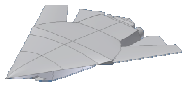

3.3 Index of Abbreviations

AAW	Active Aeroelastic Wing
CAP	Combat Air Patrol
CAS	Close Air Support
DARPA	Defense Advanced Research Projects Agency
MEMS	Micro-Electro-Mechanical Systems
NASA	National Air and Space Administration
PVDF	Polyvinylidene
RAINBOW	Reduced And Internally-Biased Oxide Wafer
RFP	Request For Proposal
SMA	Shape Memory Alloy
SWAT	Smart Wing Adaptive Technologies
TDT	Transonic Dynamic Tunnel
THUNDER	THin layer composite Unimorph ferroelectric DrivER and sensor
UAV	Unmanned Air Vehicle
UCAV	Unmanned Combat Air Vehicle
VSTOL	Vertical/Short Take-off and Landing

3.4 Index of Symbols

E	Endurance
C_L	Lift Coefficient
C_D	Drag Coefficient
W_1	Takeoff Weight
W_2	Landing Weight
W	Weight
C_t	Rate of Fuel Consumption
R	Range
	Density
$\overline{S}$	Wing Surface Area
ROC	Rate of Climb
v	Velocity
T	Thrust
D	Drag
v_{TO}	Takeoff Velocity
v_L	Landing Velocity
C_{Lmax}	Maximum Lift Coefficient
g	Gravity
AR	Aspect Ratio
e_0	Oswald Efficiency Factor
Λ_{LE}	Leading Edge Sweep Angle
C_{D0}	Induced Drag
W_0	Total Gross Takeoff Weight
W_{crew}	Crew Weight
$W_{payload}$	Payload Weight
W_e	Empty Aircraft Weight
W_f	Fuel Weight
M_{max}	Maximum Mach number
K_{vs}	Variable Sweep Constant

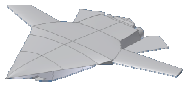

4 INITIAL CONCEPT DEVELOPMENT

4.1 Request for Proposal

This aircraft design initiative was created in response to a request for proposal (RFP) generated by the Virginia Tech Aerospace Engineering department, in conjunction with the United States Air Force. This RFP calls for the classification of methods through which an aircraft could change its configuration in-flight as well as the classification of those missions in which morphing technologies would prove beneficial. Further, the RFP requested the development and eventual detailed design of an aircraft which exploited morphing technology.

Though the theoretical benefits from morphing technologies are widely known in the aircraft industry, actual demonstrations of their validity have been limited. What this RFP calls for is the development of an aircraft which will serve, in addition to its intended mission, as a technological demonstrator for morphing technologies. The new and unorthodox technologies utilized in this aircraft will necessitate that the final aircraft outperform conventional aircraft, as persuading the potential customers to purchase the plane. The customer must be impressed enough by these benefits to offset any doubts about new and potentially more costly technologies.

4.2 Morphing Discussion

4.2.1 Introduction to Morphing

The word morphing, in respect to aircraft, means to physically change the appearance or configuration of the aircraft. Morphing technologies, considered to be the future of the aircraft industry, can greatly influence an aircraft's performance characteristics and future aircraft will ideally be able to respond continuously to varying flight conditions using technologies currently under development. This technology may likely use sensors, as nerves in a bird's wing, to

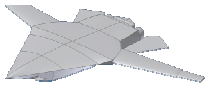

measure pressures over the entire wing surface which would then guide actuators that would function like the muscles in a bird's wing and change shape to optimize the flight conditions.

There are many types of morphing that can be done on an aircraft. Most are categorized into control morphing or mission morphing concepts. In the design approach for this project both categories were looked at thoroughly. Multiple concepts can be used in designing the most efficient aircraft possible. The following section discusses the pros and cons of each type of morphing explored and how it can best be put to use.

4.2.2 Types of Morphing

4.2.2.1 Variable Camber

The morphing technology known as variable camber is among the newest and most exciting of the morphing technologies. Its benefits include higher L/D, lower induced drag, and increased fuel efficiency. However, it does have several drawbacks including higher cost and additional weight. There are several ways that variable camber is achieved, but all have the same objective of attaining the maximum aerodynamic benefit with minimum additions to weight and cost.

Some of the main methods of producing variable camber include conventional actuators, piezoelectric materials, and shape memory alloys. Conventional actuators, also known as servos, are small devices that are use torque to help the airfoil change shape. Shape memory alloys are those materials which can return to a certain shape after being deformed. At certain temperatures, these shape memory alloys possess a low yield strength and, therefore, can be molded into a desired position which can be adjusted back to its original position.

A different concept that has recently been developed is the belt rib concept evolved by a German company named DLR. This concept replaces the previously used hinges and linear bearings with a so-called structonic solution, which uses distributed flexibility to produce the

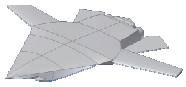

desired shape changes. The previously used classical rib is replaced by the belt rib that is able to produce local camber changes while keeping the overall stiffness of the section intact.

Flexible trailing edge structures are of high interest in variable camber designs. In these structures, the chordwise bending stiffness is acquired by the use of ribs while the spanwise bending stiffness is achieved using spanwise spars. The rear trailing edge is what is known as a "sandwich" design, in which both the upper and lower skin panels are used to form a closed profile with high torsional stiffness.

4.2.2.2 Smart Controls

Smart material controls used in place of traditional control surfaces such as flaps, ailerons, elevators, and rudder are an attractive application of morphing technologies currently being studied. The potential benefits of improved flow control include improved performance and maneuverability, affordability, increased range and payload, and environmental compliance (Kral, 1).

There are a few key things to consider when redesigning aircraft controls. Flight controls can be either active, or passive. Passive techniques of control include geometric shaping to manipulate the pressure gradient, the use of fixed mechanical vortex generators for separation control, and placement of longitudinal grooves, or riblets on a surface to reduce drag. Active controls can be predetermined, or interactive. Predetermined methods of control involve the introduction of energy steady or unsteady input without consideration for the state of the flow. Jet vectoring using piezoelectric actuators and post stall lift enhancement and form drag reduction using oscillating blowers are just a few examples of predetermined active controls. The interactive method of flow control uses sensors to continuously adjust the power to the control actuator (Kral, 1).

Whether the control is active or passive the technology of how to apply the shape changes required to manipulate the flow is very important. Beginning in the 1980's many

researchers have investigated the use of fully integrated adaptive material actuator systems for performance enhancing shape control because these devices offer significant advantage over their conventional counterparts: no flow disturbing hinge lines. The Defense Advanced Research Projects Agency (DARPA)/ Air Force Research Laboratories/National Air and Space Administration (NASA)/Northrop Grumman Smart Wing program was one such effort addressing the development and demonstration of smart technologies (McGowan, 2). The overall objective of the smart wing program was to develop smart technologies and demonstrate novel actuation systems to improve the aerodynamic and aeroelastic performance of military aircraft

There are actuators being tested and considered now that will even further change aircraft controls. Piezoelectric materials represent one of the main materials currently being investigated for application in morphing structures. The unique quality of piezoelectric materials is that they can be used as either sensors, or actuators for the controls themselves. These materials when contorted generate a voltage that could be measured and used as a sensor. Piezoelectric materials can also bend and conform when a voltage is applied to them. If this could be controlled it could be used to deflect the trailing edge and control the aircraft (McGowan, 2).

Piezoelectric materials come in several varieties. Piezoelectric polymers work as a function of the materials dipole concentration. Fluoropolymers like polyvinylidene (PVDF) are at the forefront. These polyimides are of key interest because of their high temperature stability and ease with which polar pendant groups may be incorporated. The aircraft morphing project is looking at potential use of piezoelectric polymidied in Micro-Electro-Mechanical Systems (MEMS) devices, as fluoroploymers do not possess the chemical or thermal stability necessary to withstand normal MEMS processing (Simpson, 3).

Piezoelectric materials also come in high displacement ceramic actuators. Piezoelectric devices have been identified as a promising actuator technology for the implementation of flow control. The problem is that many aerospace applications require displacements greater then what is achievable with conventional piezoelectric. Recently though Langley Research Center

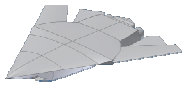

(LaRC) researchers have developed two high displacement piezoelectric actuator technologies. RAINBOW (Reduced And Internally-Biased Oxide Wafer) and THUNDER (THin layer composite Unimorph ferroelectric DrivER and sensor) are uniform actuators, which consist of piezoelectric ceramic layer bonded to one or more non-piezoelectric secondary layers. Due to elevated temperatures used during processing internal stresses are created in the structure, which significantly enhance displacements through the thickness of the device (Simpson, 3).

The main drawbacks of piezoelectric materials are their high excitation voltage needed to work. Some other problems are the mechanical durability of these materials have small strain values (Uchino, 4) and also their ability in coupling the material to the control system and structure is uncertain.

Materials that change their shapes when exposed to magnetic fields can now be used to drive high-reliability linear motors and actuators. When a piece of Terfenol-D is placed near a magnet, the special rare-earth iron material will change shape slightly. This remarkable phenomena, called the magnetostriction effect, has been the focus of efforts by engineers to devise a simple, high reliability linear motor based actuator (Ashely, 5).

4.2.2.3 Adaptive Torque Control

Adaptive torque control is a control morphing concept that is designed to reduce flutter at high speeds. Torque is defined as a measurement of turning or twisting force applied to an object. As a result, applying a moment across the axial member will cause twisting in the wing, increase roll rates at high speeds and help eliminate roll reversal. An actuator can be used with piezoelectric torque-plates, which actively twist or deform in response to an applied electric field. The base of the plate is firmly attached to the airframe while the tip is attached to an aerodynamic shell that rotates about a main spar. Another way to apply torque control which has been tested and proven is through the use of shape memory alloy torque tubes. In this application the wing

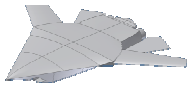

ribs would be furnished with integral tangs that have firm fitting slots in the torque tube connecters to allow transmission to twist to several sections of the wing.

4.2.2.4 Adaptive Aeroacoustics

Adaptive aeroacoustics is an idea that has stemmed from research aimed at pinpointing the source of sounds that are generated during aircraft flight. More particularly, it is focused on the aerodynamic and structural sources of sound as opposed to those produced by the power plant. This includes attenuation of interior noise in aircraft fuselages, active and passive damping of structural vibrations, shape and vibration control of space vibrations, and active control of aeroelastic flutter (Gibbs, 6). Though it would be useful to develop this type of technology for commercial applications, it would probably be more suitable for military applications, in particular aircraft that have stealth characteristics.

A substantial amount of noise generated by large military aircraft, such as bombers, results from adverse pressure and velocity distributions stemming form turbulent flow over a structure (Pinkerton, 7). In most cases, this takes place in locations that are not aerodynamically sound such as landing gear doors, control surfaces, and most importantly bay doors used to deliver large weapons. The application of adaptive aeroacoustics around the bay doors for bombers or strike aircraft is the focus of this morphing research. This technology would modify the shape of the structure to make the flow less turbulent through the open bay Bearing in mind that aircraft such as the B-2 are based on stealth characteristics for effectiveness, minimizing noise would greatly improve the value of such hardware for the Air Force. Shape memory alloys allow the shape of the bay doors to change upon actuation thus modifying the shape of the region around the door to counter turbulent noise.

The main drawback with this type of technology is its inherently high cost for relatively small benefit. It would only be worth the cost on a very limited number of applications. These

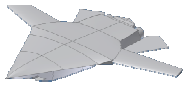

applications will almost all be military related and will probably already incorporate some degree of stealth capability.

4.2.2.5 Adaptive Drag Rudders

Adaptive drag rudders are a result of research intended to come up with a morphing concept that would provide a means of yawing an aircraft without the need for vertical control surfaces used in conventional aircraft (Erickson, 8). To solve this problem it is required that some sort of a force be generated on the wing in either the direction of or opposite the thrust. To come up with a solution for this problem, a number of different methods have been suggested. One of them would involve a spoiler to create drag, creating an excess of drag on one wing and causing yaw. The aim of this technology is to accomplish the same task while giving away as little as possible insofar as visibility is concerned.

Adaptive bumps are essentially bulges that are created on either wing in order to create drag, having a part of the top (or bottom) surface pop outwards over what was initially a smooth wing. This roughness causes the flow to become turbulent and depending on the size and number of bumps, it may even separate. The change from laminar to turbulent flow causes a rapid increase in drag. Note that since this drag is on one of the two wings, a yawing moment will be created.

One of the ways in which this can be accomplished is by having a fluid (either some sort of hydraulic liquid or air) drive a piston that is placed inside the wing. The piston can move up or down based on an input signal (which can take the form of an electric signal or a change in temperature that would expand gas placed inside the cylinder). Since the tip of the piston would be connected to the skin of the aircraft, it would be possible to extend the skin upwards thus creating a small bump. When required, the piston could be pushed back down thus bringing the skin back into place and creating laminar flow over the wing.

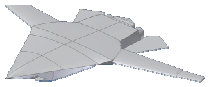

Another means of delivering the same result would be by having a shaft-like extension that extends outwards from the skin. The top of the shaft would of course be the same shape as the skin so that when not extended, the flow will behave as if nothing was there to cause any disturbances. When extended, there will be a shaft that juts out from the skin. Since this impedes the flow of air moving over the wing, the resulting turbulent flow on one side thus causing yaw. The cylinder can then be drawn back using the same means that were used to extend it in the first place

Once again, as with most morphing concepts, there is a significant limit in applications where adaptive drag rudders can be used. Much like variable winglets could only be used with wings of large span and aspect ratio; this can only be used in tailless aircraft. Moreover, this has little application outside of military uses and is most likely to be used in long range bombers or UCAVs currently under development.

4.2.2.6 Variable Winglets

Variable winglet technology is a morphing concept that has arisen from the success seen in the use of winglets for aircraft with relatively large wingspans and aspect ratios. In particular, winglets are in wide use today in the commercial airliner market with such aircraft as the Boeing 747-400 and the Airbus A330 and A340 making use of this concept. Here, researchers are looking to develop a wing that can utilize the great benefits achieved from a winglet placed on the tip without giving up the advantages that are present in an aircraft wing that has a large span and aspect ratio but does not have a winglet. The latter characteristic is present among gliders and other low speed and high endurance aircraft (Montoya, 9). As with all morphing technologies the reason for blending these two technologies is to allow for a wider range of benefits throughout the flight envelope.

A number of viable candidates are present to accomplish this task. The first concept is one that would probably be mechanically more complex than the second but probably simpler to use and

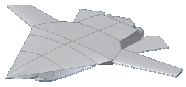

design. It would basically consist of a set of gears (similar to cogs in shape) that would rotate in such a manner that the angle the winglet makes with the spar of the wing could be manipulated. This would not be too dissimilar from conventional flaps. The only main difference would be that instead of having a part of the wing change in the direction of the airflow, it would move axially.

The second possibility uses a combination of smart materials that essentially compose the wingtip. Results have been obtained with smart materials similar to those achieved using purely mechanical devices or sets of devices. On the other hand, due to the lack of complexity in such a design, it would be much simpler to design the parts that go into the wingtip. As of now, this type of material actuation being used in a wingtip is entirely new. Furthermore, it is still unclear how much energy would be needed to fold the tip back and forth whereas a relatively good idea on the power requirements for a mechanical wingtip can be derived from conventional controls

4.2.2.7 Telescopic Wing

The telescoping wing is a mission morphing concept where an overlapping spar system is used to increase the wingspan of an aircraft. The wing extension/retraction controls can be simpler than that of a normal flap. The control can either be switched to the extended or retracted position.

The telescopic wing has many advantages to that of a normal wing. This wing morphing has a component of versatility that a normal wing does not have. The advantages of having the wings retracted are that it reduces drag, which in turn improves speed and efficiency. Hanger space can be minimized as well as that the small wing area provides a higher quality of flight through violent air. In the retracted position the wing has a higher stiffness and resistance to twist. Some advantages of having the wings extended are that the rate of climb is improved as are the endurance, range, and absolute ceiling of the aircraft. Takeoff and landing speeds and takeoff and landing lengths are also reduced with the wings extensions (Gevers Aircraft, 10).

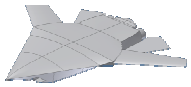

The main drawbacks of telescoping wing technologies lie in the increased mechanical requirements within the wing. Not only do added mechanical systems increase the weight of the aircraft, they would also decrease the amount of fuel which could be stored within the wing otherwise. Potential interactions between the telescoping wing and other morphing technologies must also be considered.

4.2.2.8 Variable Geometry Swing Wing

Swing wing technology is a mission morphing concept currently used on numerous multi-mission aircraft. The swing wing provides versatility to an aircraft, allowing sweep angle and aspect ratio to be adjusted in flight for optimum positions for each particular speed regime. The swing wing pivot would be located outboard of the fuselage with a highly swept glove extending from the pivot to the side of the fuselage. In this application of variable sweep the rearward neutral point shift is minimized. Current swing wing designs have several different sweep positions which the aircraft utilizes through the use of a sweep schedule to greatly increase the flight envelope.

Each sweep position has its advantages at certain flight speeds and conditions. The near zero sweep angle presents a high aspect ratio that would be suitable for takeoff and landing, and for better climb rates. The intermediate sweep positions would be used in normal flight conditions such as cruise at subsonic speeds. At high subsonic and supersonic speeds the aircraft would operate best with the wings fully swept.

4.2.2.9 Fowler Flaps

Fowler flaps are a high lifting device that provides additional lift by increasing the wing area, increasing the camber, and accelerating the airflow between the wing and the flap. Fowler flaps increase the maximum lift coefficient and also have lower drag at the maximum Cl compared to other flaps.

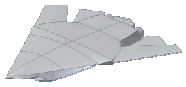

Fowler flaps are different from regular flaps because they have a gap between the deflected flap and the main part of the wing. They also move backwards, which increases the wing area, as well as deflect down. Traditional flaps are simply connected to the trailing edge of the wing and deflect down but do not move backwards. The internal design of fowler flaps allows for retraction of the flaps at high speed flight. The flap is moved out and back in using a series of tracks and rollers.

4.2.2.10 Variable Tip Dihedral

Variable tip dihedral is similar to a variable winglet but is different in two main aspects. First of all, it is usually applied to aircraft that fly at very high (in excess of Mach 2) speeds. Secondly, it is applied to a greater portion of the wing area than the first concept. The way in which it works is very similar to a variable winglet. That is, a mechanical device is installed in the wing that allows it to fold back and forth. In many ways, this is similar to a standard flap in the manner in which it is actuated.

Its main purpose is to alter the location of the aerodynamic center at very high speeds. This was the primary purpose as to it being installed on the XB-70. Additionally, its shape takes advantage of the shock that is formed below the wing at very high speeds. Due to the shape of the wing, the aircraft is partially supported on this shock, which allows the aircraft to fly further distances for a given speeds and fuel load.

4.3 Initial Mission Development

4.3.1 Brainstorming Session

After determining the beneficial aspects of each of the morphing technologies, it was necessary to develop mission types which would benefit from one or a combination of several these technologies. Upon the conclusion of a brainstorming session it was found that the majority of the missions listed fell under one of three mission types: surveillance, transport, or attack.

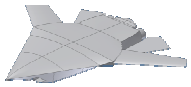

4.3.2 Downselection

One mission from each of the three initial types was developed for further consideration. For each, type a mission profile was created from either Federal Aviation Regulation or Military Requirement specified profiles. After the missions were developed, they were compared on six different criteria: technological benefits, demonstration quality, user need, versatility, wow factor, and feasibility. The technological benefit factor took into account the ways and relative amounts in which the basic mission parameters would be increased over the status quo.

The basic goal of this design initiative is to develop an aircraft and mission package which would best demonstrate the benefits of morphing technology it is important to assess which missions would better demonstrate this. Thus it is important to asses the demonstration quality of each mission. Need was also taken into account in terms of potential customer desire and consumer return investment. While it is important to demonstrate a benefit for a specific mission, it is also important to demonstrate the multi-mission enhancing capabilities of morphing technologies, which falls under the criteria of versatility.

Finally, the amount in which the user is 'wowed' by the mission capabilities of the concept and the ability to actually accomplish the mission goals were taken into account. Each of these criteria were ranked in the decision process to select a single mission type for further development.

4.3.2.1 Short Takeoff Transport

Due to the potentially large economic benefits that even tiny increases in fuel economy can have for transport users the morphing benefits in this area were heavily considered. Though shorter takeoff and landing capabilities would also allow commercial carriers to operate larger aircraft out of smaller airports, this benefit would be more important for military aircraft operating in forward support roles.

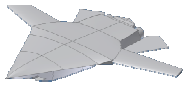

The transport concept was determined to be the most feasible mission; however, it was also found to be the least versatile, have the least consumer need, and have the lowest demonstration quality of each of the examined mission types.

4.3.2.2 Fighter/Attack UCAV

The main drawback of developing a morphing aircraft for a transportation mission lies in the desire for multi-mission capabilities of the aircraft. The required configuration for a transportation aircraft does not lend itself for easy conversion into a fighter. Since multi-mission capabilities were high on the list of desirable traits of a morphing aircraft, military missions were subsequently developed. The first mission which was considered was a fighter/attack mission profile.

The fighter/attack role is currently fulfilled by aircraft such as the F/A-18 Hornet and the F-15 Eagle. Though capable of fulfilling both missions each of these aircraft are biased, through design limitations, towards either the fighter or attack mission. The application of morphing techniques would allow for an unbiased approach to both missions at the same time.

Two missions were developed for this aircraft type: medium range attack and close air support. These would be the extreme cases which this aircraft would need to meet, with any combat air patrol or other fighter roles falling between the scopes of these two missions. The first, the medium range attack, requires a longer range and higher speeds than the close air support mission. Alternatively, the close air support requires better maneuverability at low speeds.

Though less feasible than the transport mission, this set of mission capabilities increases the versatility of an aircraft designed to fulfill these requirements. This mission could also better utilize more types of morphing technologies, creating a larger benefit from morphing and at the same time a higher morphing demonstration quality.

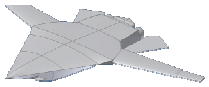

4.3.2.3 Surveillance – Quick Attack UCAV

While aircraft with high altitude and long loiter capabilities have been used for surveillance missions for many years, only recently have these aircraft begun being employed in attack missions as well. The mating of a hellfire missile system with a Predator UAV created the first operational UCAV, as well as the first long loiter reconnaissance aircraft with strike capabilities. Without morphing technologies, the use of a missile is the only feasible way to have a surveillance aircraft attack a previously stalked target. Were it possible for the aircraft to change into a higher speed configuration, it could dive down from its surveillance post and attack and retreat at high speeds utilizing bombs instead of missiles. Thus, the surveillance – quick attack mission was developed.

A change in aircraft configuration is required to maintain optimum capabilities in both mission regimes. As previously stated, most aircraft would be capable of performing both aspects of this mission separately, but the aircraft would not be well suited for both missions. The versatility and demonstration quality of an aircraft fulfilling this mission profile would be higher than those of a transport aircraft, but lower than one meeting an attack/fighter profile.

4.4 Initial Concepts

At the onset of the mission development phase, two initial aircraft concepts were developed for each mission. it was decided that each of the concepts fulfilling the military missions be Unmanned Air Vehicles (UAVs) due to the required control systems complexity and the increasing desire for their use in the military. Certain characteristic constraints were assigned to each concept prior to initial development. The main characteristics of each concept and which mission it was designed for are found in Table 4.1.

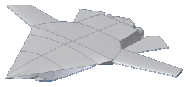

Table 4.1: Initial Concept Descriptions

Transport Mission	
Conventional Transport	Variable camber, smart controls
Blended Wing Transport	Variable winglets, variable camber, smart controls, adaptive drag rudders
Fighter/Attack Mission	
Conventional Fighter/Attack	Variable camber, smart controls
Forward Swept – VSTOL	VSTOL capabilities, variable camber, smart controls, adaptive torque control, adaptive drag rudders
Recon – Quick Attack Mission	
Telescoping Wing Recon	Telescoping wing, variable camber, smart controls, adaptive torque control
Swing Wing Recon	Swing wing, variable camber, smart controls, adaptive torque control

Once a mission was selected, further concept development was needed to accurately assess all the morphing possibilities and their benefits. The mission chosen was the Fighter/Attack profile. A total of eight initial concepts were looked at for further development. The two concepts initially proposed to fill the mission parameters were refined and six new concepts were created under the following guidelines. Three of the six new aircraft were designated to be tailless and thus used adaptive drag rudder technology. Two concepts were designed for VSTOL capabilities, two with swing wings, and two with telescoping wing technology. The resulting eight aircraft concepts and their attributes are listed in Table 4.2.

Table 4.2: Fighter/Attack Mission Specific Concepts

Fighter/Attack Mission	
Forward Swept	VSTOL capabilities, variable camber, smart controls, adaptive torque control
Conventional	Variable camber, smart controls
Concept 3	Tailless, swing wing, variable camber, smart controls, adaptive torque control, adaptive drag rudders
Concept 4	VSTOL capabilities, swing wing, variable camber, smart controls, adaptive torque control
Concept 5	Tailless, telescoping wing, variable camber, smart controls, adaptive drag rudders, adaptive torque control
Concept 6	VSTOL capabilities, telescoping wing, adaptive torque control, variable camber, smart controls
Concept 7	Tailless, conventional design, variable camber, adaptive drag rudders, smart controls
Concept 8	Conventional design, variable camber, smart controls

Those concepts which were very similar to other designs were removed along with those which were of lesser quality. After this down selection, four concepts remained for further consideration.

The first of the final four concepts was the forward swept VSTOL concept. Seen in Figure 4.1, this concept, designated SWAT–1, is a tailless concept featuring a forward swept wing and lifting canards. The VSTOL scheme utilized in this concept is a hybrid-fan lifting system with axisymmetric thrust vectoring. The morphing technologies inherent in this concept are variable camber, adaptive smart controls, and adaptive torque control.

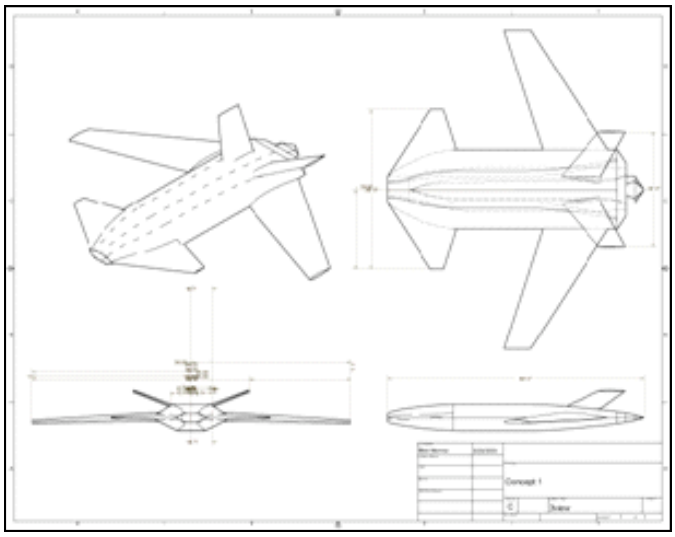

Figure 4.1: SWAT–1, Forward Swept VSTOL Concept

The next concept considered, designated SWAT-2, was a tailless swing wing concept. This aircraft, seen in Figure 4.2, utilizes conventional swing wing technology as a form of mission morphing. The control morphing technologies found in this concept include variable camber, adaptive smart controls, adaptive torque control, and adaptive drag rudders.

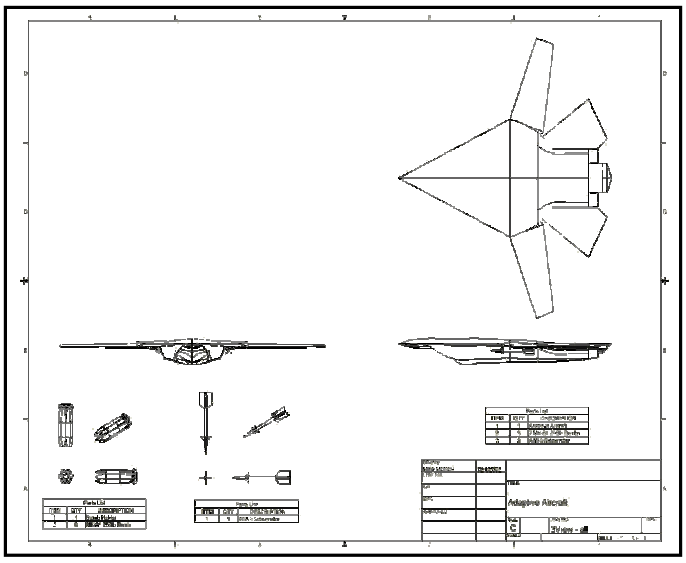

Figure 4.2: SWAT-2, Tailless Swing Wing Concept

Telescoping wing technology is featured as the mission morphing technology in the third concept. This concept, seen in Figure 4.3 as SWAT-3, features a largely trapezoidal wing with forward lifting canards. For VSTOL capabilities this concept utilizes a center fuselage lifting fan as well as thrust vectoring for added control. Control morphing technologies included in this design are variable camber, smart controls, and adaptive torque control.

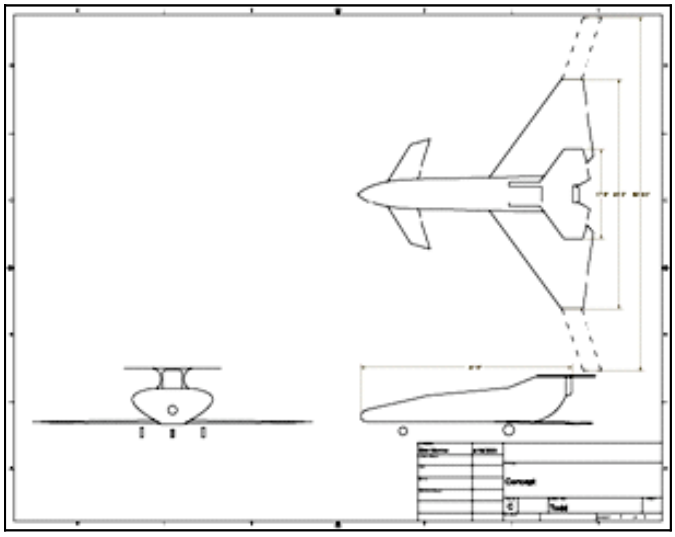

Figure 4.3: SWAT-3, Telescoping Wing Concept

Finally, SWAT-4, the conventional concept featuring no mission morphing technology is seen in Figure 4.4. This concept solely features control morphing in the form of variable camber, smart controls, and adaptive torque control.

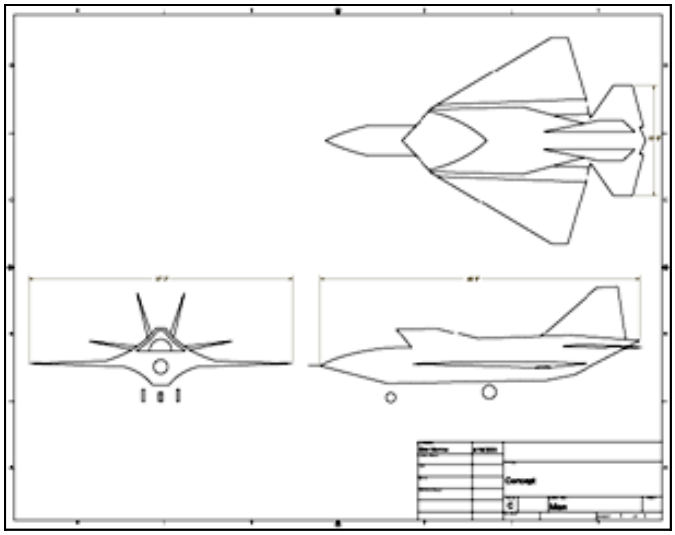

Figure 4.4: SWAT-4, Conventional Design Concept

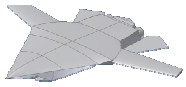

5 CONCEPT ANALYSIS AND SELECTION PROCESSES

5.1 Mission Selection

5.1.1 Mission Decision Matrix

The selection of a single mission for further development was conducted through the use of a decision matrix. The factors considered included the benefit from morphing technology, the demonstration quality, current need for that type of aircraft, mission versatility, feasibility, and the wow factor. The results of the decision matrix analysis are found in Table 5.1.

As seen in the second row of the matrix, the maximum available score in this case was 100, with benefit and demonstration quality respectively being 30 and 25. In this analysis, the transport mission faired the worst with a score of 56. With a score of 71, the reconnaissance mission was only slightly surpassed by the fighter/attack mission. From this analysis, the fighter/attack mission was chosen for further development and use in the final aircraft concept design.

Table 5.1: Aircraft Mission Decision Matrix

Mission Decision Matrix	*Benefit*	*Demonstration*	*Need*	*Versatility*	*Wow*	*Feasability*	*Total*
Max Available	30	25	15	15	10	5	100
Transport	25	10	8	5	3	5	56
Reconnaissance	25	15	12	10	6	3	71
Fighter/Attack	27	20	12	13	8	1	81

5.1.2 Mission Refinement

Once a desired mission type was selected, refinement of this mission type was required. Department of Defense officials have expressed the interest of the Air Force in a smaller and cheaper medium range bomber for their next bomber purchase (Asker, 11). This aircraft would

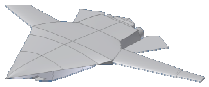

be required to carry a payload of 16-20 small diameter 250 lb. bombs. One of the scenarios put forth by military officials, invasions several of these smaller UCAV bombers taking the place of fewer large bombers in attacking targets.

Further design of the attack/fighter concepts has been centered on this request. Since this is not the only mission in consideration, further ordinance were selected. In addition to sixteen 250 lb. Mk 81 bombs, the concepts will carry 2 AIM-9X sidewinder missiles and a M61A1 cannon system. This configuration is only for the Hi-Lo-Lo-Hi medium strike mission and will change for the other different mission requirements.

5.2 Morphing Type Selection

5.2.1 Morphing Decision Matrix

After the selection of the fighter/attack mission, it was necessary to determine which morphing technologies would be best utilized in carrying out the mission requirements. A decision matrix system was utilized using similar ranking parameters. In this case seven parameters were looked at, including mission benefit, newness of the technology, application versatility, technology cost, maintenance, ease of pilot use, and 'wow' factor. For comparison purposes the technology in question was compared with the conventional technology it would replace.

For the technology decision matrix, the most important factors were the benefit over the status quo and the ability to use the technology for different missions. The technology was considered for application over different missions at this stage due to the fact that this aircraft is to be a technology demonstrator. As seen in Table 5.2, the technologies which achieved the two highest score were the smart material controls and variable camber.

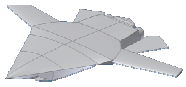

Table 5.2: Morphing Technology Decision Matrix

Technology Decision Matrix	*Benefit*	*New?*	*Versatility*	*Cost*	*Maintenance*	*Ease of Use*	*Wow*	*Total*
Max Available	30	5	20	15	15	10	5	100
Smart Materials Controls	18	4	19	11	12	8	3	75
Camber Change	23	5	19	5	10	1	4	67
Fowler Flaps	16	2	10	14	14	9	0	65
Torque Control	15	5	9	12	14	3	2	60
Variable Winglets	9	5	12	9	11	9	2	57
Aeroacoustics	8	5	15	8	12	6	2	56
Telescoping Wing	17	4	11	2	7	9	4	54
Adaptable Drag Rudders	10	5	7	8	13	7	3	53
Swing Wing	13	1	9	13	8	7	1	52
Variable Tip Dihedral	13	3	5	7	9	7	3	47

5.3 Concept Downselect

5.3.1 Concept Decision Matrix

Concept selection was also conducted through the use of decision matrix analysis. In this situation, as seen in Table 5.3, the benefit over currently used aircraft and the demonstration quality of the concept were considered to be the most important aspects of this decision. Prior to conduction of the concept analysis all VSTOL qualities of the concepts were discarded. It was decided that any VSTOL capabilities would be attempting to accomplish the same goals as morphing technologies used to shorten take-off and landing distances. Thus VSTOL technology would be detrimental to any morphing technology demonstrations. The conventional and forward swept designs acquired the least number of points through the decision matrix method, leaving the telescoping wing and swing wing concepts. It was decided that since the telescoping wing and swing wing concepts were relatively close in score that a more detailed concept analysis was required for decision between these two concepts. This process is described in detail in the next section.

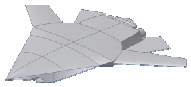

Table 5.3: Aircraft Concept Decision Matrix

Concept Decision Matrix	Benefit	Versatility	Designability	Wow	Demonstration	Feasability	Total
Max Available	30	5	15	5	25	20	100
Swing Concept	25	3	10	3	20	16	77
Telescoping Concept	25	5	5	5	20	9	69
Forward Swept	15	3	8	4	15	12	57
Conventional	10	1	12	1	10	17	51

5.4 Final Concept Selection

5.4.1 Comparative Aircraft Study

Before a concept selection was made, detailed comparisons of the two final concepts were conducted. Aircraft properties not directly derived from the concept's geometry, such as weight ratios, available thrust, and overall lengths, were estimated from other aircraft currently fulfilling similar missions. A comparative study of similar modern aircraft was conducted, but was eventually narrowed down to the fifteen aircraft seen in Table 5.4.

Table 5.4: Current Aircraft Used For Initial Comparisons

Strike and Close Support Aircraft					
A-10	Su-39	Alpha Jet	AMX	Su-22	Tornado
Multi-Role Aircraft					
AV-8B	F-14D	F-111	F-18E	F-15E	F-16C
Su-24	Mig-27	Yak-38			

Of these fifteen aircraft, six are swing wing aircraft and two are VSTOL aircraft. These aircraft were selected because they exhibited characteristics similar to those which will be present in the final concept. The remaining nine aircraft were used for comparative purposes because, they are currently used by various countries to perform the missions selected.

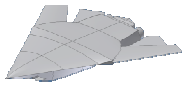

All aircraft properties which could be derived from concept geometry, such as wing span, wing area, and aspect ratio, were measured and calculated from the conceptual drawings assuming an overall length of 46' for initial sizing purposes.

5.4.2 Sizing Comparisons

Initial sizing and weight comparisons were computed using Nicolai's Aircraft Sizing Algorithm v0.9, which is part of the Virginia Tech Aerospace Software Series. The algorithm was run with the geometrically derived aircraft properties and the design ordinance load determined from the Department of Defense suggestions.

To obtain the total gross take off weight, the final inputs of a 250 nm strike radius and a cruise speed of Mach 0.9 were entered. This combination of properties resulted in an estimated total gross take off weight of 40,000 pounds and an empty weight of 25,000 pounds.

5.4.3 Performance Analysis

Selection between the two final concepts was decided through a quantitative comparison of aircraft performance. For this comparison a flight condition was set arbitrarily at 30,000 ft with at Mach 0.9. Some other fixed parameters used in the comparisons were the weight, thrust, fuel consumption rate, the maximum lift coefficient, and the parasite drag.

The comparison was done using a performance spreadsheet developed in to calculate each of the performance values. Performance characteristics such as takeoff and landing properties, range, and endurance were studied because the aircraft geometry alone had a significant effect on their values. The performance equations utilized for these calculations include the following:

$$E = \frac{1}{\square_T} \frac{C_L}{C_D} \ln\left[\frac{W_1}{W_2}\right] \qquad (6.1)$$

$$R = \frac{V}{c_T}\frac{C_L}{C_D}\ln\left(\frac{W_1}{W_2}\right) \tag{6.2}$$

$$RC = \left(\frac{T - D}{W}\right)V \tag{6.3}$$

$$v_{TO} = 1.2 * \sqrt{\frac{2 * W_1}{\rho * S * C_{L_{\max}}}} \tag{6.4}$$

$$S_{TO} = \frac{1}{2B}\ln\left(\frac{A}{A - BV_{TO}^2}\right) \tag{6.5}$$

$$S_L = \frac{1}{2B}\ln\left(1 - \frac{B}{A}V_L^2\right) \tag{6.6}$$

$$v_L = 0.91 * \sqrt{\frac{2 * W_2}{\rho * S * C_{L_{\max}}}} \tag{6.7}$$

$$A = g\left(\frac{T_o}{W} - f\right) \tag{6.8}$$

$$B = \frac{g}{W}\left(\frac{1}{2}\rho S\left(C_D - fC_{Lg}\right) + a\right) \tag{6.9}$$

Equation 1 is the endurance equation, c_t is the rate of fuel consumption, C_L and C_D are the lift and drag coefficients, which in this case were equivalent to maximum L/D, and also in the equation are W_1 the takeoff weight and W_2, the landing weight. Equation 2 is the range equation the C_L in this equation is different from the normal C_L, the equation for the C_L to maximize range is shown below. Also in the range equation, ρ is the density at altitude. Equation 3 is the rate of climb equation, v is the velocity, T is the thrust, D is the drag, and W is the weight. Equations 4 and 6 a similar they are the takeoff and landing velocities with the ρ here being the density at sea level, S is the area of the wing, and C_{Lmax} is the maximum value of the lift coefficient. Equations 5 and 7 are solved for the takeoff and landing distances. Again the ρ in these equations is the

density at sea level, g is gravity, f_{TO} is 1, and h is equal to 50. In equation 7, n i9s 0.1, gamma is 0.1, and a equals 0.45g.

Table 5.5 shows the final performance numbers for each concept. Two configurations were selected to cover the full range of the aircraft's potential; however, the configuration will be changing to further maximize the aircraft's performance. The highlighted cells correspond to the best result of each particular performance parameter with the yellow cells representing SWAT-2 and the orange representing that the advantage belongs to SWAT-3. No, obvious winner in terms of overall performance, in response the SWAT-5 was developed as a version of the SWAT-2 with a telescoping wing section.

When the wings of the SWAT-5 are un-swept, the wing would be capable of telescoping to a new span of 68 ft. This new configuration still does not have better field performance than the SWAT-3 concept, but is an improvement over the SWAT-2.

Table 5.5: Performance Analysis Results

Performance Analysis Results	range	endurance	rate of climb	take-off distance	landing distance
units	nm	hours	ft/s	ft	ft
SWAT-2	4140.388	7.713	380.704	2774.231	6800.778
SWAT-2 swept	2577.354	4.144	337.379	2195.477	4904.361
SWAT-3	3241.073	6.026	364.813	2341.576	5333.875
SWAT-3 telescoped	3053.597	6.928	360.740	1758.522	4118.128
SWAT-5 telescoped	3573.474	6.568	371.321	2398.8176	5949.2027

5.4.4 Decision Matrix

In order to compare the results from the performance comparison, a comparative method was utilized, in which each of the concepts was compared to the Swing Wing Concept. In this method five performance characteristics were considered equally, these were: range, endurance, maximum rate of climb, take-off distance, and landing distance. The values, determined in the

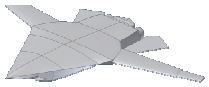

performance analysis for each concept, were compared with the values found for the swing wing concept. The resulting comparisons were then averaged for final comparison.

Through this method, the results of which are found in Table 5.6, it was found that though the telescoping wing concept had poorer range and endurance characteristics, the differences in take-off and landing distances added to make this aircraft an all around better choice than the Swing Wing Concept. The blended concept of a swing wing and a telescoping wing had equal values in the range and endurance categories and better qualities in take-off and landing distances, though not as good as the telescoping wing, but the combination of all the qualities led to the blended concept being a better all around design.

Table 5.6: Performance Decision Matrix

Performance Decision Matrix	*Range*	*Endurance*	*Take-Off Distance*	*Landing Distance*	***Overall***
SWAT-2	1.00	1.00	1.00	1.00	1.00
SWAT-3	0.78	0.90	1.25	1.19	1.03
SWAT-5	1.00	1.00	1.16	1.14	1.07

5.5 Refined Concept

5.5.1 Mission

The concept selected will be required to meet a variety of different mission profiles. A total of four design missions have been selected in an attempt to demonstrate the multi-mission capabilities of this design. The most demanding of these profiles will be the Hi-Lo-Lo-Hi medium range strike mission. The three other profiles used to assess the final concept include Combat Air Patrol (CAP), Close Air Support (CAS), and Recon-Quick Strike missions. This blend of missions was chosen because it spans the variety of missions a true multi-mission aircraft will be required to perform.

5.5.2 The SWAT-5 Mako

The final concept selected was the blended swing wing/telescoping wing concept. Figure 5.0 shows the final SWAT-5 concept, nicknamed the Mako. Note that the aircraft features both swing wing and telescoping wing technologies. The tip chord of this concept is 4', and the telescoping section used in the performance evaluation was a 3' chord section 8' in length which extends at the same sweep angle as the main wing. The basic geometry, sizing, and design ordinance characteristics of this aircraft are listed in Table 5.7.

There are five morphing technologies featured on this concept. The mission morphing technologies are swing wing and telescoping wing technologies. Control morphing technologies utilized include variable camber, adaptive smart controls, and adaptive torque control.

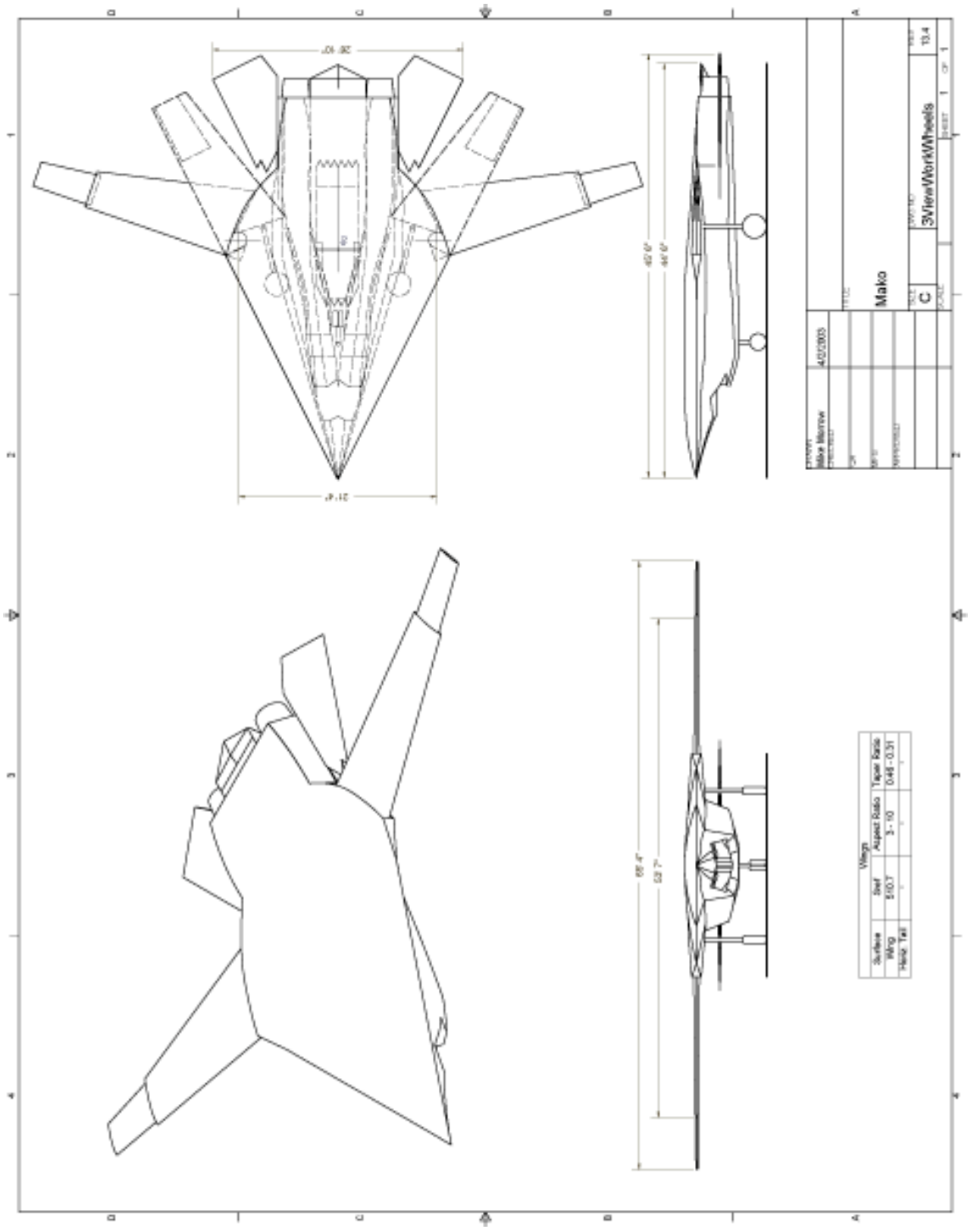

Figure 5.0: SWAT-5 Mako

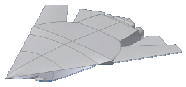

Table 5.7: Final Concept Characteristics

SWAT-5 Mako Characteristics

Geometry	
Length	45.5 feet
Height (without gear)	5 feet
Span (Unswept)	56 feet
Span (Swept)	42 feet
Span (Telescoped & Unswept)	68 feet
Reference Wing Area	573 square feet
Aspect Ratio	8.551
Reference Chord	11 feet
Sweep Angle (Unswept)	19 deg
Sweep Angle (Swept)	63.3 deg
W/S	64.6

Sizing	
Empty Weight	21,300 lbs.
Take-Off Gross Weight	37,000 lbs.
Payload Weight	5500 lbs.
Fuel Weight	10,000 lbs.
Available Thrust	35,400 lbs.
T/W	0.95

Design Max Ordinance Load	
(2) AIM-9X	380 lbs.
(16) Mk 81 Bombs	4160 lbs.
M61A1 Cannon System	500 lbs.

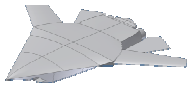

6 MISSION AND PERFORMANCE

6.1 Performance

Performance issues are very important to the SWAT-5 design because it is intended to compete and outperform existing aircraft.

6.1.1 Takeoff Analysis

A takeoff analysis following the procedure described in Raymer was conducted in order to provide the details of the aircrafts takeoff performance (Raymer, 12). Using the equations discussed in the initial performance evaluation, it was determined that the takeoff distance was approximately 2250 ft with a corresponding takeoff velocity of 246.45 ft/s. In this analysis _, the ground rolling, resistance was taken to be 0.03, which is the common value for dry concrete/asphalt. The takeoff distance, however, can be reduced to 1791 ft with the telescoping wing section. The telescoping wing increases wing area and span to allow the aircraft to takeoff in a shorter distance with less velocity.

6.1.2 Landing Analysis

The landing distance of an aircraft is calculated, again, in the un-swept position to allow for maximum lift and, therefore, a slower descent into landing in a shorter distance. The landing distance for the un-swept configuration was found to be approximately 4850 ft with a corresponding landing velocity of 249.45 ft/s. This distance can once again be reduced with the use of the telescoping section to a lower value of 4252 ft, with an approach speed of 286.9 ft/s.

6.1.3 Cruise Analysis

The aircraft is expected to cruise at a mach number of 0.9. Assuming that the aircraft would be cruising with the wings swept, this would imply a C_L of 0.44 (at an altitude of 40,000

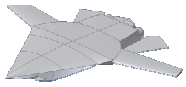

ft). The required thrust-to-weight ratio would then be 0.082. The aircraft can expect to achieve a maximum rate of climb of approximately 48,727 ft/s at sea level at the takeoff weight of approximately 37,000 lbs, which is comparable to fighter aircraft such as the F-14 and F-16.

6.1.4 Range and Endurance

The expected range, if the aircraft were to be maintained at cruise altitude and speed is determined from the Breguet range equation. Because the aircraft will be involved in a number of different mission segments (e.g. climb, cruise-in/out, dive, etc.) it is essential to brake the mission into 500nm segments and then use the Brequet range formula on each segment to determine the effective range of the aircraft.

With an expected specific fuel consumption of 1.85 and a decrease in weight from 40 000 lbs to 25 000lbs the range of this aircraft in the forward wing swept position would be 3072nm. It must be noted, however, that this value only applies if the aircraft were to maintain straight and level flight throughout the duration of the mission. Conversely, the range in the swept wing configuration would only be 1768nm due to the decrease in L/D. Un-swept wings would be the ideal configuration while hoping to maximize range and fuel consumption. At a cruise altitude of 40,000 ft. with the aircraft in the un-swept configuration the expected maximum endurance is 7.2 hours.

6.1.5 Rate of Climb

The maximum rate of climb versus altitude plot, found in Figure 6.1, was developed using the method (Raymer, 12). The plot illustrates the decline of the maximum attainable rate of climb with increasing altitude and increasing weight. Figure 6.1 shows the rates of climb in the un-swept and telescoped configuration, which allows the highest rate of climb.

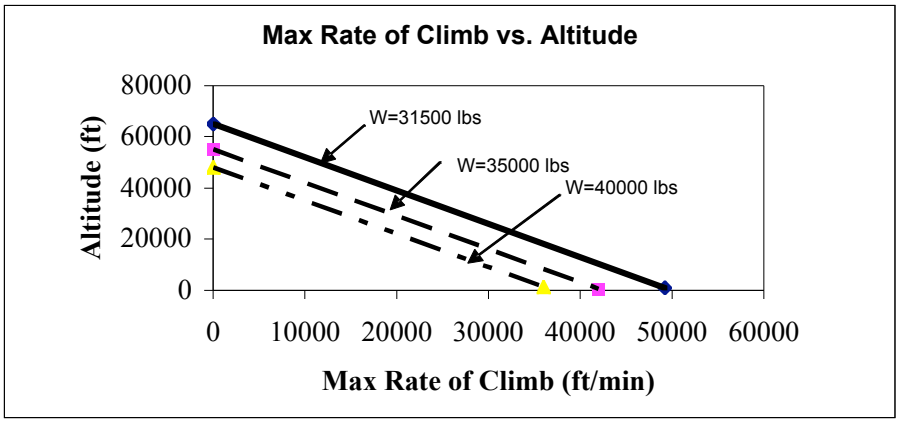

Figure 6.1: Rate of climb versus altitude

It was found that the aircraft could not sustain a rate of climb of 1,000 ft/min above an altitude of approximately 54,000 ft, making this altitude the supersonic combat ceiling of the aircraft. The service ceiling, defined as the altitude at which the aircraft cannot maintain a rate of climb of 100 ft/min was found to be 61,000 ft.

6.1.6 Benefits of Morphing Technology

Table 6.1 was made to demonstrate the benefits that could be achieved by including morphing technologies such as variable sweep and a telescoping wing section. The chart clearly shows a decrease in takeoff and landing distance when in the un-swept configuration, and an even greater decrease with the telescoping extension. The landing distance, for instance, decreased from 5831ft in the normal 40 degree sweep position to 4850ft in the wing swept position, which is a 17% decrease. Then, when including telescoping wing there is 17% decrease from the wing swept position. Results are similar for takeoff distance. The maximum rate of climb at sea level also shows a significant increase as the wings are moved closer to the un-swept position.

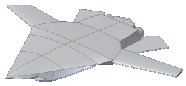

Table 6.1: Performance Comparison

Sweep	*Cl*	*Max Rate of Climb (ft/s)*	*Takeoff Distance (ft)*	*Landing Distance (ft)*	*Range (nm)*	*Endurance (hours)*
20	0.48	48,657	2,237	4,838	4,190	7.75
20 w/tel	0.43	46,209	1,776	4,261	4,016	7.55
30	0.47	48,306	2,362	4,722	3,353	7.15
40	0.45	47,317	2,489	5,817	3,157	6.41
50	0.4	44,861	2,712	6,231	2,925	5.62
60	0.37	41,371	2,888	6,618	2,715	4.66

Table 6.1 assumes the cruise altitude and mach number of 40,000ft and 0.9, respectively for C_L calculations, while rate of climb calculations assume sea level altitude and constant thrust. Further analysis resulted in the resulting benefits found in Table 6.2.

Table 6.2: Morphing benefits comparison

Mission	*Factor*	*Value*		*Increase over 40°*
		40°	*Variable*	
Combat Air Patrol	Loiter	116	150	29%
Close Air Support	Radius	216	250	16%
Recon / Quick Strike	Loiter	201	270	34%
Medium Range Bomber	Radius	289	350	21%

6.1.7 Carpet Plot

A carpet plot was created to assess the ability of the SWAT-5 to meet the required specifications. This plot was created using the initial sizing methods described in "Aircraft Design: A Conceptual Approach" (Raymer,12). Chapter 6 in Raymer contains the following relations:

$$W_0 = \frac{W_{crew} + W_{payload}}{1 - \left(\frac{W_f}{W_0}\right) - \left(\frac{W_e}{W_0}\right)} \tag{6.10}$$

$$\frac{W_e}{W_0} = \left[a + b W_0^{C1} A^{C2} \left(\frac{T}{W_0}\right)^{C3} \left(\frac{W_0}{S}\right)^{C4} M_{\max}^{C5} \right] K_{vs} \tag{6.11}$$

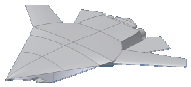

where W_0 is the total gross take off weight, W_{crew} is the weight of the crew, $W_{payload}$ is the weight of the payload, W_f is the weight of the fuel, W_e is the weight of the empty aircraft, A is the aspect ratio, T is the thrust, S is the planform area, M_{max} is the max mach, and K_{vs} is the variable sweep constant. The constants a, b, and C1 through C5 are determined based on the type of jet aircraft. In the case of the refined concept, the variable sweep constant is 1.04 to increase the empty weight ratio based on the increased mechanics of the sweeping wings.

To generate the carpet plot seen in Figure 6.1, the thrust to weight ratio and the wing loading were varied in equation 6.11. To apply constraints, the performance equations were solved for the wing loading for a range of thrust to weight ratios. This allowed equations 10 and 11 to be solved for the total gross take off weight. These constrain lines were plotted by comparing them to values on the carpet plot and interpolating in between them to determined exact locations. Since the aircraft has multiple configurations, the carpet plot was adjusted to account for the ability of the wings to change their leading edge sweep angle. After obtaining the wing loading, it was adjusted by the ratio of the planform area of the wings un-swept to the planform area of the wings swept. After this adjustment was made, the constraint lines were added to the carpet plot.

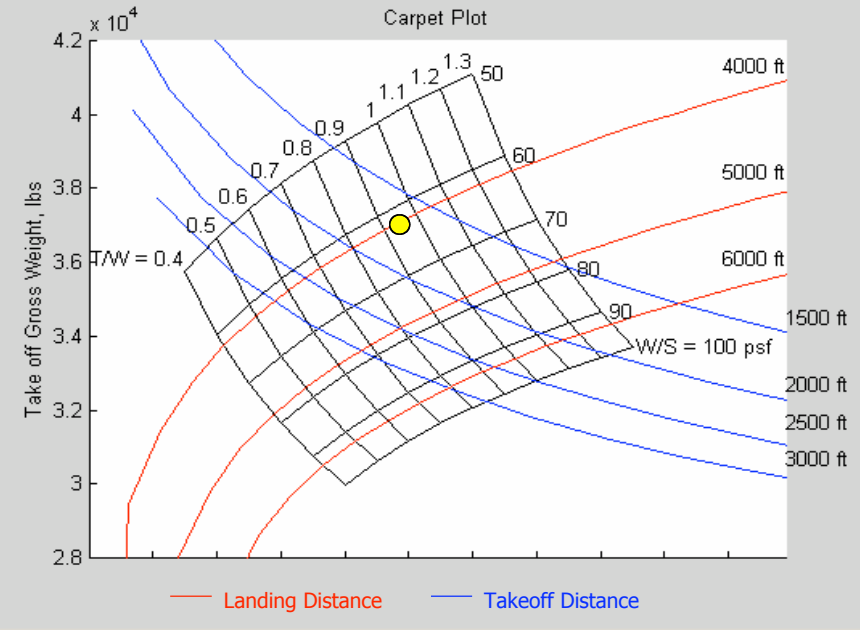

Figure 6.1: Final Concept Carpet Plot

6.1.8 Specific Excess Power

A major indication of an aircraft's performance ability is the amount of specific excess power, or Ps, that it has at any given time. Ps is a very important performance characteristic, and even a 50 ft/s increase in Ps is considered a major advantage is high maneuverability situations such as dogfights. The values of Ps for four different load factors, seen in Figure 6.2, are representative of the aircraft at 30,000 feet in the un-swept configuration.

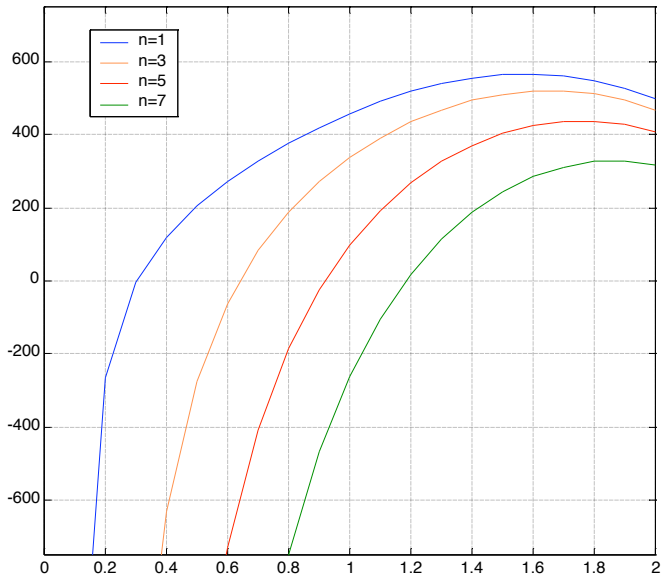

Figure 6.2: Specific excess power

The available power decreases as the load factor increases, as a higher load factor means more drag and thus less power. Note, also, that Ps = 0 for n = 5 at Mach = 0.9 at 30,000 feet. This is a "meet or exceed" point for fighter aircraft, meaning that this value of Ps has to be met or exceeded for the aircraft to be successful.

6.2 Mission

As previously mentioned the mission capabilities of the SWAT-5 Mako were analyzed for four different missions: Medium Range Strike, Combat Air Patrol, Close Air Support, and Recon-Quick Strike.

6.2.1 Medium Range Strike

The most demanding of these missions is the medium range strike, for which a Hi-Lo-Lo-Hi profile was chosen. The major aspects of the medium range strike profile, seen in Figure 6.3, are the 250 nm cruise at 40,000 and Mach 0.9 followed by a 50 nm low level penetration run at Mach

0.8. The second half of the profile is basically a mirror image of the first half with a low level egress and 40,000 ft cruise return to base for a total range of 1000 nm.

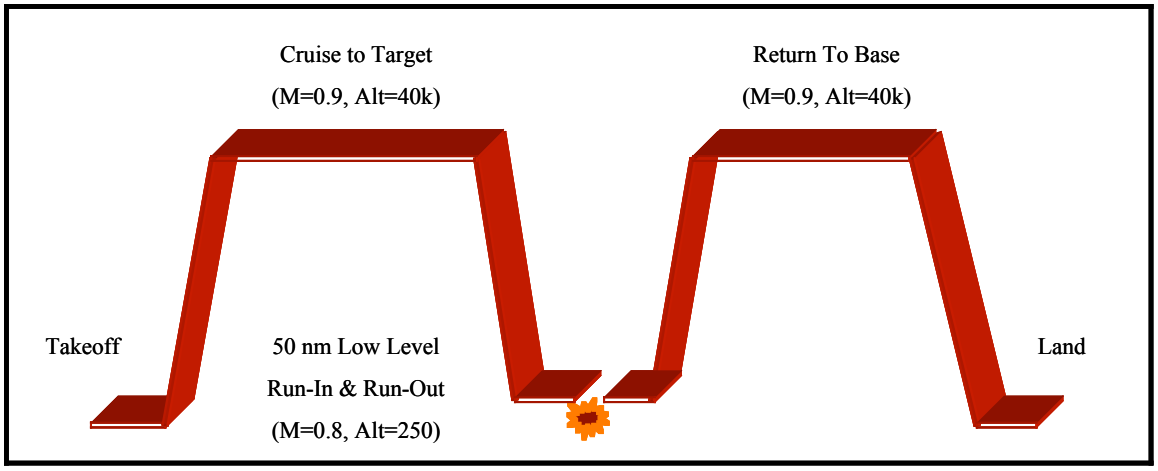

Figure 6.3: Hi-Lo-Lo-Hi Medium Range Strike Mission Profile

The design ordinance load for this configuration is 5,660 lbs., the contents of which are found in Table 6.3. The base ordinance load consists of the M61A1 cannon system with 1,000 rounds along with 2 AIM-9X Sidewinder missiles carried partially submerged under the fuselage. For this mission a maximum of 12 250 lb. small diameter bombs can be carried on two rotor dispensers in the weapons bay. Additionally 6 250 lb. small diameter bombs can be carried in sets of three on under strake pylons on missions where stealth is not as large a consideration. This option brings the capabilities to the level suggested by the Department of Defense.

Table 6.3: Medium Range Strike Design Ordinance Load

Medium Range - Strike

Max Weight:	***Internal:***	***External:***	
5660 lbs	*(1) Cannon (kind not determined yet)*	*(2) AIM-9X*	*(Partially sunk in fuselage)*
	(12) 250 lb small diameter bombs	*(0-6) 250 lb small diameter bombs*	*(Under strake pylons)*

The mission program developed by Michael Morrow was utilized to determine whether the SWAT-5 would meet the requirements for this mission (Morrow, 13). The results are detailed in Table 6.4.

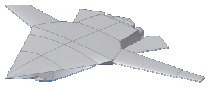

Table 6.4: Medium range strike mission program results

Mission Profile: Medium Range Strike

Segment	Description	Altitude ft	Distance nm	Time min	Time hr	Total Fuel lbs	Section Fuel lbs
1	Warm Up/Taxi	0	0	0	0.00	10230	0
2	Take-off and accelerate to climb speed	0	0	20	0.33	8897	1333
3	Climb on courcse to cruise altitude	35000	21	22.3	0.37	7944	953
4	Cruise to start of penetration	35000	371	67.9	1.13	5492	2452
5	Descend to Sea level	500	371	67.9	1.13	5492	0
6	Run-in specified distance at sea level to target	500	421	73.5	1.23	4709	783
7	Drop Stores	500	421	73.5	1.23	4709	0
8	Attack Target	500	421	73.5	1.23	4709	0
9	Run-out specified distance at sea level from ta	500	471	79.2	1.32	3927	782
10	climb on course to cruise	35000	489	81.2	1.35	3131	796
11	cruise to base	35000	839	127	2.11	912	2219
12	arrive over base with reserve fuel	35000	839	127	2.11	912	0
13	Loiter	500	839	137	2.28	600	312
14	Land/Taxi/Shut Down	0	839	137	2.28	0	600
	Percent Reserve Fuel	0.05865					

6.2.2 Combat Air Patrol

A basic mission requirement for a fighter aircraft is that of the Combat Air Patrol (CAP). In the mission profile found in XXX consists of a 40,000 ft. cruise at Mach 0.9 to the patrol area where the aircraft will then descend to a patrol altitude of 35,000 ft. and loiter for 1 hour and then engage the enemy. The return to base brings the mission range to 400 nm.

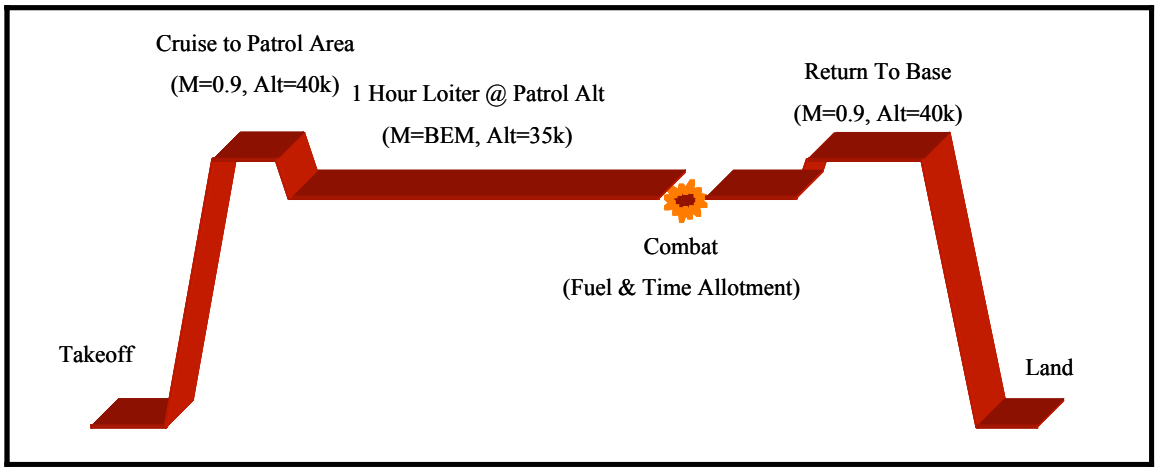

Figure 6.3: Combat Air Patrol Mission Profile

The design ordinance load for this configuration is 2,990 lbs., the contents of which are found in Table 6.4. Along with the base ordinance load the maximum mission load consists of 2 internally

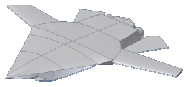

carried AIM-120 AMRAAM missiles. Additionally 4 more AMRAAM's may be carried in sets of two on the under strake pylons.

Table 6.4: Fighter Design Load

Fighter			
Max Weight:	***Internal:***	***External:***	
2990 lbs	*(1) Cannon (kind not determined yet)*	*(2) AIM-9X*	*(Partially sunk in fuselage)*
	(2) AIM-120 AMRAAM	*(2-4) AIM-9X or AIM-120*	*(Under strake pylons)*

The results of the mission program for this mission are detailed in Table 6.5.

Table 6.5: Combat air patrol mission program results

Mission Profile: Combat Air Patrol

Segment	Description	Altitude ft	Distance nm	Time min	Time hr	Total Fuel lbs	Section Fuel lbs
1	Warm Up/Taxi	0	0	0	0.00	10230	0
2	Take-off and accelerate to climb speed	0	0	20	0.33	8897	1333
3	Climb on course to cruise altitude	35000	21	22.3	0.37	7085	1812
4	Cruise to patrol area	35000	171	41.9	0.70	6881	204
5	Descend to patrol altitude	30000	171	41.9	0.70	6881	0
6	Loiter for 150 mins	30000	171	192	3.20	1710	5171
7	Drop Stores	30000	171	192	3.20	1710	0
8	Combat	30000	171	192	3.20	1710	0
9	climb on course to cruise	35000	175	192	3.20	1599	111
10	cruise to base	35000	325	212	3.53	668	931
11	arrive over base with reserve fuel	35000	325	212	3.53	668	0
12	Loiter	0	325	222	3.70	357	311
13	Land/Taxi/Shut Down	0	325	222	3.70	0	357
	Percent Reserve Fuel	3.49%					

6.2.3 Close Air Support

The Close Air Support mission required the aircraft to carry large ordinance loads to support ground forces while still retaining good maneuvering capabilities. In this mission, the profile of which is found in Figure 6.4, consists of a Mach 0.9 cruise to the target at 15,000 ft. followed by a low level loiter for 1 hour also at Mach 0.9 and then a Mach 0.8 attack run. The total mission distance for this profile is 400 nm.

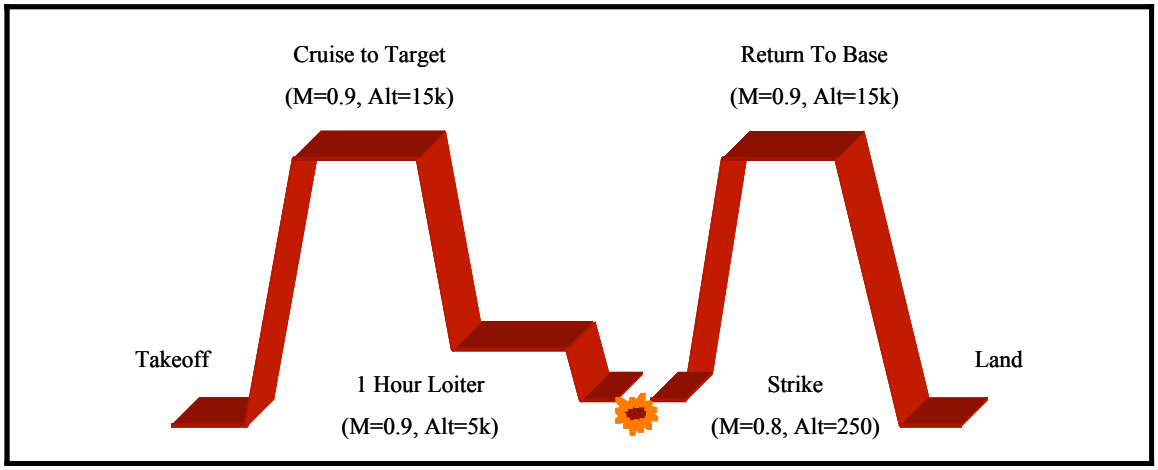

Figure 6.4: Close Air Support Mission Profile

The design load for this configuration is a total of 5,450 lbs. consisting of the base payload, 6 250 lbs. small diameter bombs, and up to 6 AGM-65 Maverick missiles. The layout of this load can be seen in Table 6.6.

Table 6.6: Close Air Support Ordinance Load

Close Air Support

Max Weight:	***Internal:***	***External:***	
5450 lbs	*(1) Cannon (kind not determined yet)*	*(2) AIM-9X*	*(Partially sunk in fuselage)*
	(6) 250 lb small diameter bombs	*(2-4) AGM-65 Maverick Missiles*	*(Under strake pylons)*
	(2) AGM-65 Maverick Missiles		

The results of the mission program for this mission are detailed in Table 6.7.

Table 6.7: Close air support mission program results

Mission Profile: Close Support

Segment	Description	Altitude ft	Distance nm	Time min	Time hr	Total Fuel lbs	Section Fuel lbs
1	Warm Up/Taxi	0	0	0	0.00	10230	0
2	Take-off and accelerate to climb speed	0	0	20	0.33	8897	1333
3	Climb on courcse to cruise altitude	15000	6	20.7	0.34	8493	404
4	Cruise to start of penetration	15000	256	50.6	0.84	5893	2600
5	Descend to Sea level	5000	256	50.6	0.84	5893	0
6	Loiter for 1 hour	5000	256	111	1.84	3737	2156
7	Drop Stores	5000	256	111	1.84	3737	0
8	Attack Target	5000	256	111	1.84	3737	0
9	climb on course to cruise	15000	262	111	1.85	3405	332
10	cruise to base	15000	512	141	2.35	881	2524
11	arrive over base with reserve fuel	15000	512	141	2.35	881	0
12	Loiter	0	512	151	2.52	566	315
13	Land/Taxi/Shut Down	0	512	151	2.52	0	566
	Percent Reserve Fuel	5.53%					

6.2.4 Recon-Quick Strike

The Recon-Quick Strike mission requires that the aircraft carry a small ordinance load and stay aloft for a long period of time while performing the reconnaissance mission and then be capable of attacking a target. The mission profile, seen in Figure 6.3, is based off of a Navy Anti-Submarine Warfare mission profile which requires the aircraft to cruise to a patrol area, loiter for four hours and then deploy it's ordinance. The design mission range for this profile is only 500 nm with an elapsed mission time of six hours.

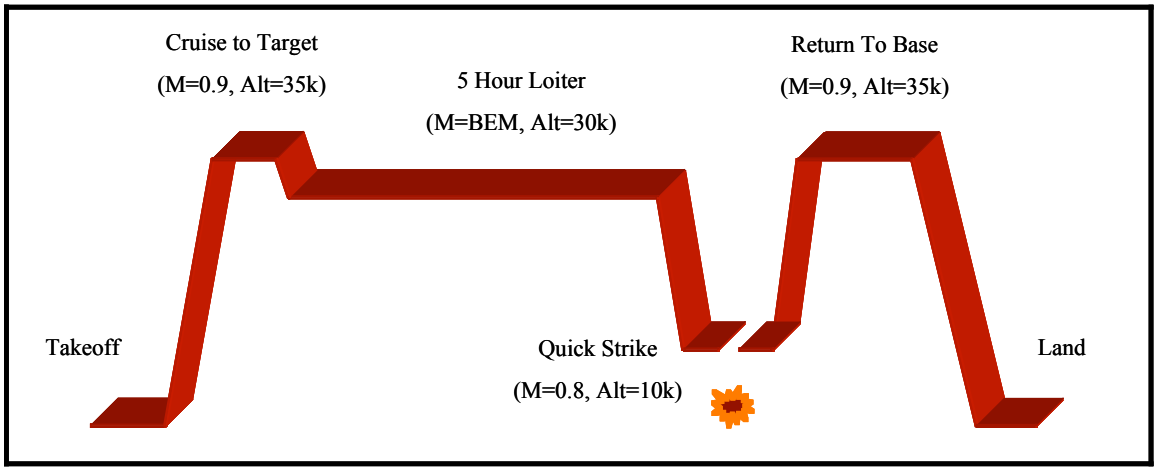

Figure 6.5: Recon-Quick Strike Mission Profile

The design ordinance load found in Table 6.8 consists of 6 250 lb. small diameter bombs and 2 1,000 external fuel tanks in addition to the base ordinance. For this mission 3,000 lbs. of fuel will also be added inside the weapons bay in place of unnecessary ordinance. This will bring the total fuel to the needed 15,000 lbs. for the loiter mission.

Table 6.8: Recon-Quick Strike Ordinance Load

Recon - Strike

Max Weight:	***Internal:***	***External:***	
4540 lbs	*(1) Cannon (kind not determined yet)*	*(2) AIM-9X*	*(Partially sunk in fuselage)*
	(6) 250 lb small diameter bombs	*(2) 1000 lb external drop tanks*	*(Under strake pylons)*

The results of the mission program for this mission are detailed in Table 6.9.

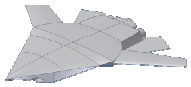

Table 6.9: Recon-Quick Strike mission program results

Mission Profile: Recon-Strike

Segment	Description	Altitude ft	Distance nm	Time min	Time hr	Total Fuel lbs	Section Fuel lbs
1	Warm Up/Taxi	0	0	0	0.00	15334	0
2	Take-off and accelerate to climb speed	0	0	20	0.33	14001	1333
3	Climb on courcse to cruise altitude	35000	21	22.3	0.37	12998	1003
4	Cruise to patrol area	35000	271	59	0.98	11366	1632
5	Descend to patrol altitude	30000	271	59	0.98	11366	0
6	Loiter for 4 hrs 30 min	30000	271	329	5.48	2261	9105
7	Descend to attack altitude	500	271	329	5.48	2261	0
8	Attack Target	500	271	329	5.48	2261	0
9	climb on course to cruise	35000	285	331	5.51	1618	643
10	cruise to base	35000	535	369	6.15	377	1241
11	arrive over base with reserve fuel	35000	535	369	6.15	377	0
12	Loiter	0	535	379	6.32	113	264
13	Land/Taxi/Shut Down	0	535	379	6.32	0	113
	Percent Reserve Fuel	0.74%					

7 AERODYNAMICS

Due to the fact that the SWAT-5 design is capable of morphing the aerodynamic characteristics need to be looked for a variety of configurations. When typically designing a fighter there are certain criteria which the aircraft must meet. This usually means the aircraft performs better a certain flight conditions rather then others, thus limiting the aircraft to specific missions. The SWAT-5 Mako is designed to have optimal aerodynamic and flight performance at both high and low speeds. In order to do this first the planform area was analyzed and compared to historical data.

7.1 Planform Selection

The planform of the SWAT-5 is variable because the wing is variable sweep and has the ability to telescope to add area and span. Historical data shows that certain aspect ratios and taper ratios are better for different speeds. Table 7.1 shows planform historical trends alongside of the SWAT-5 planform data (Raymer, 12).

Table 7.1: Comparison of SWAT-5 Mako and historical data

Historical Data	
Low Sweep Wings	
Taper Ratio	0.4 - 0.5
Aspect Ratio	8.0 - 9.0
Swept	
Taper Ratio	0.2 - 0.3
Aspect Ratio	2.0 - 4.0
F-15	
Taper Ratio	0.25
Aspect Ratio	3

SWAT Team	
Unswept	
Taper Ratio	0.4048
Aspect Ratio	10.17
Swept	
Taper Ratio	0.409
Aspect Ratio	3.03

The aspect ratio and taper ratio have important influences on wing loading and other important aerodynamic effects. The first planform shown is the telescoped wing at 19° sweep. This is a long slender wing with a high aspect ratio (Figure 7.1).

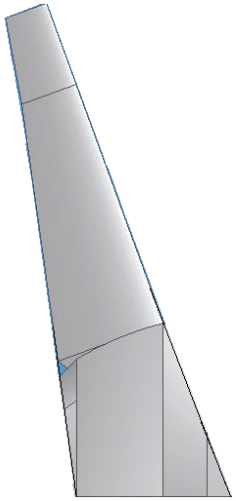

Figure 7.1: 19° sweep with the telescoping section extended

This wing would be used where high lift is needed say for take-off, landing, and certain missions where a long loiter time may be required. The next planforms are the wing at 19° sweep without the telescope extended and also the wing swept completely back at 63.4° (Figure 7.2). Depending on the aircrafts speed the sweep could be anywhere between, or at these to two shown conditions.

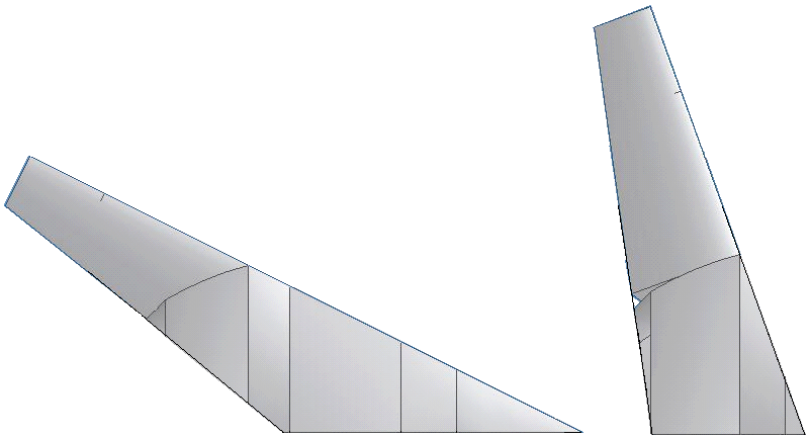

Figure 7.2: 19° sweep without telescoping section extended and swept completely back at 63.4°

At a high angle of sweep there is no need to have a sharp leading edge which allows the wing to be thicker. This is important for this aircraft because thicker wings are better at slower speeds and with all the materials going into the wings internal space, thickness will be very important.

7.2 Airfoil

This is a variable camber wing, which will allow for optimal airfoil shapes at both high and low speeds. Cambered airfoils will be used for takeoff, landing, and at low speeds when more lift is needed. As the aircraft speeds up the wing could lessen the camber to zero percent for better high-speed cruise. The high sweep angle of the wing means that the leading edge of the wing does not have to be sharp to avoid shocks. This as mentioned before is important to the design of the wing structure.

Initial plans for the exact airfoil are based on lift performance and other aerodynamic properties of existing NACA airfoils. The low speed airfoil being considered is the NACA 23012 (Figure 7.3).

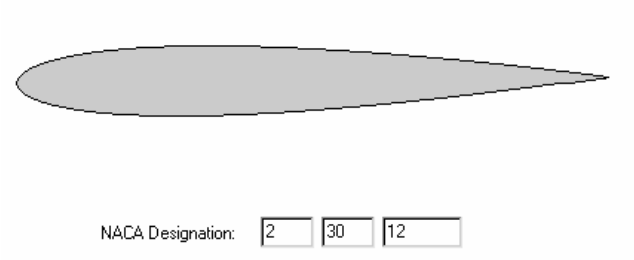

Figure 7.3: NACA 23012 airfoil. Picture from (www.desktopaero.com/appliedaero/airfoils1/airfoilgeometry.html)

This airfoil has a max C_l of 1.79 and lift curve slope of 0.104 per degree. The NACA 23012 is best used in the 185 to 200 miles per hour range of flight speeds. For higher cruise speeds the airfoil could reduce the amount of camber to zero making the airfoil close to a NACA 0012 (Figure 7.4).

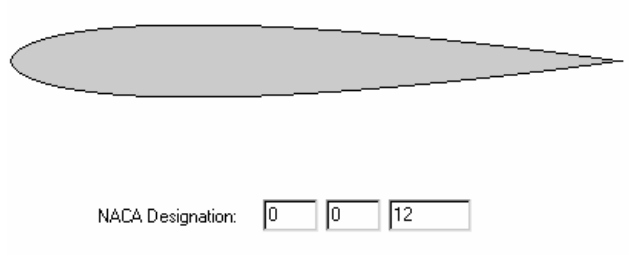

Figure 7.4: NACA 0012 airfoil. Picture from (www.desktopaero.com/appliedaero/airfoils1/airfoilgeometry.html)

In addition with the wings swept back the chord is increased, thus decreasing the *t/c* ratio of the wing making the wing appear thinner in the flow (Kress,14).

7.3 Sweep Schedule

The ability to change the sweep of the wing is desirable for many reasons: the ability to control the wings bending moment, and the wide range of Mach numbers that can be flown at efficiently. The wings, in the un-swept position, are swept 19° and can be swept back to any angle up to 63.4°. There are some important aerodynamic properties to look at when determining a sweep schedule (Kress, 14). The maximum lift-to-drag ratio as a function of Mach number is plotted for six different sweep configurations (Figure 7.5).

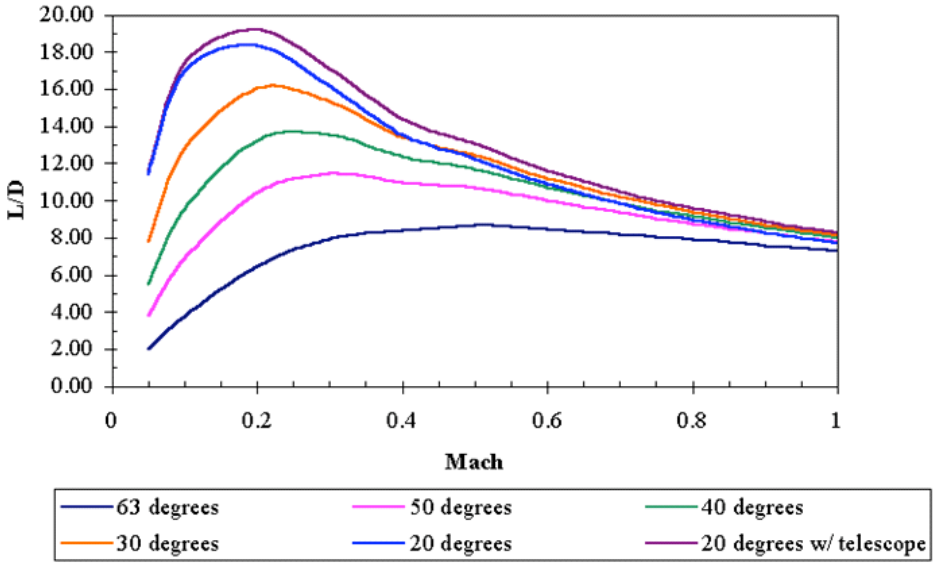

Figure 7.5: Effect of sweep on L/D

From the plot, it can be seen that as the sweep angle of the wing increases, the maximum L/D decreases. This result is mainly due to the effects of span loading with the change in sweep angle shown in Figure 7.6.

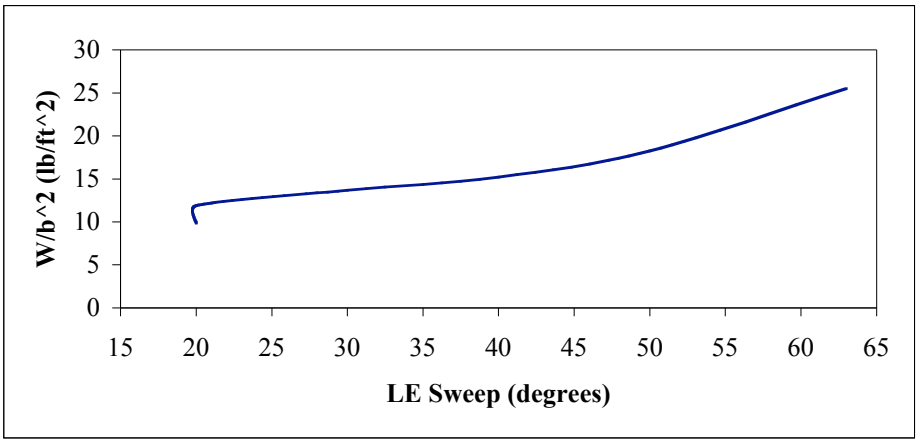

Figure 7.6: Effect of sweep on spanload

Another important property affected by the variable sweep is the zero lift drag of the aircraft. The friction and the form drag that make up the zero lift drag were found using the Friction program, while transonic and supersonic considerations where solved for in AWAVE. The effects of sweep in delaying the drag rise become extremely important in the transonic range of Mach numbers (Figure 7.7).

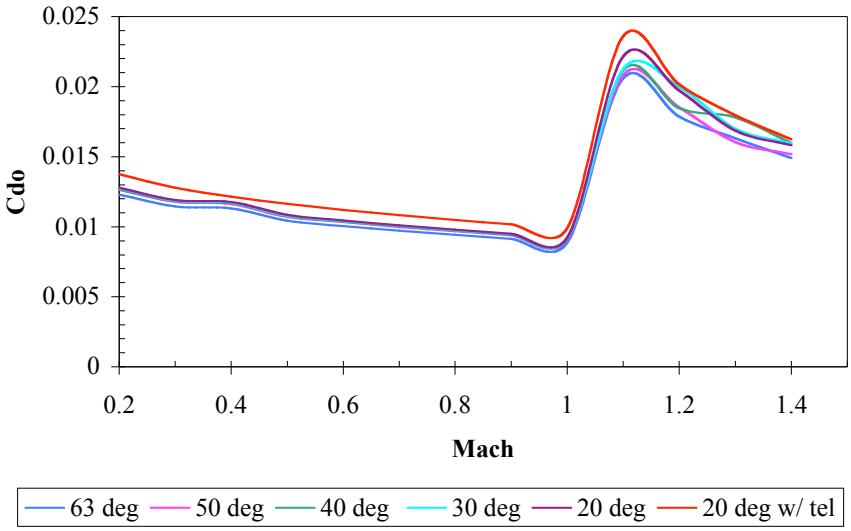

Figure 7.7: Parasite drag buildup at cruise altitude of 40,000 ft.

A fixed wing program was concluded based on the critical Mach number of each sweep angle. The critical Mach numbers were found by first using the modified Korn equation to find the drag divergence Mach number for each angle and from there the following equation was used to find the critical numbers: $M_{crit} = M_{dd} \left[\frac{0.1}{80} \right]^{1/3}$ (Mason,15). The results are show in Figure 7.8.

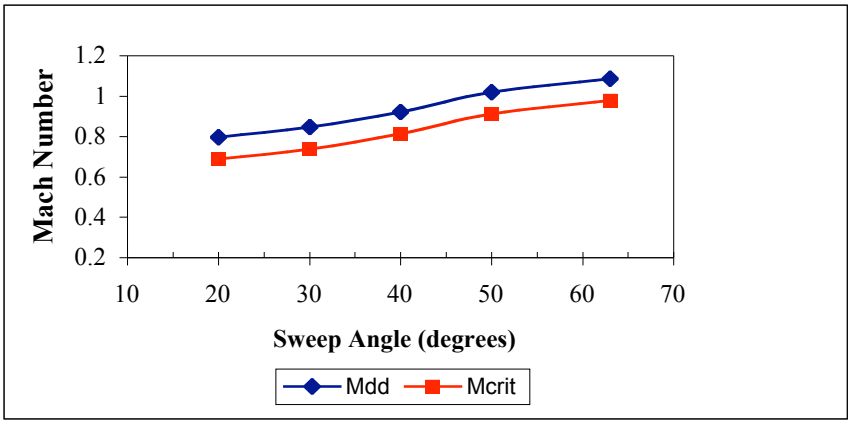

Figure 7.8: Plot of Mdd and Mcrit for various sweep angles.

The wing sweep program takes effect at mach 0.689, which is the critical Mach number for the un-swept wings. After this Mach number the sweep of the wings will adjust according the schedule shown in Figure 7.9. The critical Mach number should be as high as possible to allow

the aircraft to cruise at a high speed without a severe penalty for drag. For the SWAT-5 the critical Mach number with the wings fully swept back is 0.978. The cruise speed for this aircraft is Mach 0.9, which can be met with 50-degree angle of wing sweep without a severe drag penalty.

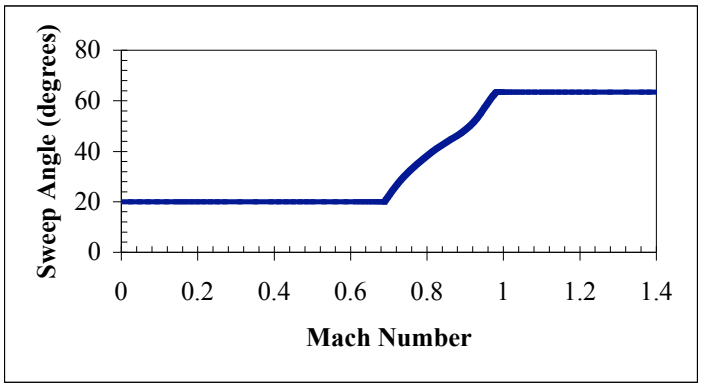

Figure 7.9: SWAT-5 Sweep Schedule

The need though for the higher wing sweep of 63° will be used at supersonic flight and also when stealth is required.

7.4 Drag Analysis

An important part of the aerodynamic considerations of the SWAT team aircraft is the build up of drag at different speeds and to find out what configuration will work best to reduce that build up. The cd_o of the aircraft was found by using two programs the first being the Friction/Form Factor Drag program and for supersonic analysis AWAVE was utilized. The Fiction program requires the aircraft be entered in terms of it's wetted area. To do this accurately the aircraft was separated into five different sections: the nose, the fuselage, the inboard wing, the outer wing, and the horizontal tail. The total wetted area was calculated to be 1,915 square ft. AWAVE was used to find the wave drag produced by the aircraft. AWAVE works by using the volume distribution of the aircraft.

To find the total drag coefficient the induced drag was calculated over a range of C_L at the cruise speed of Mach 0.9. After calculating $C_{L\square}$ and C_L for the whole aircraft for each configuration over a range of angle of attack the C_L values were plugged into $k_1 C_L^2$. Here

$k_1 = \frac{1}{\pi e_o AR}$, with e_o being Oswald's efficiency factor and AR being the aspect ratio. The total drag on the SWAT-5 fighter was then calculated using $C_D = C_{D0} + k_1 C_L^2$ (Brandt,16). With all the lift and drag coefficients found a drag polar was constructed to show the effect that sweep has on the plot. The plot was done over a range of –2 to 15 degrees angle of attack. The things that stand out are the reduction of drag with high sweep, and conversely the high lift produced while un-swept.

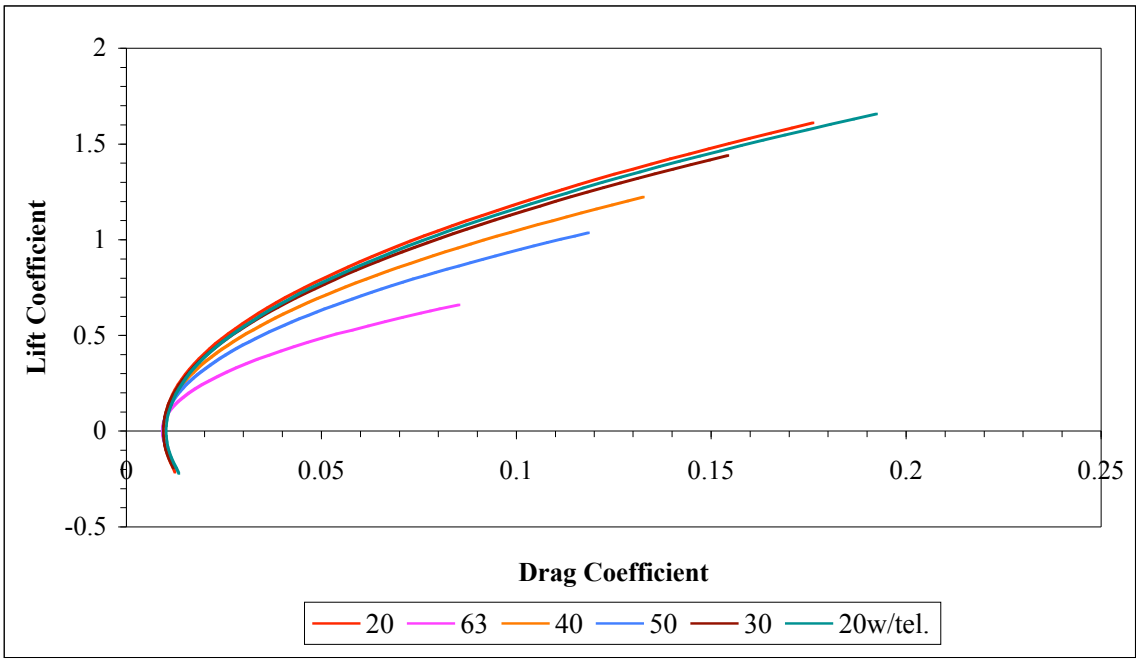

Figure 7.10: SWAT-5 Drag polar at cruise speed of Mach 0.9 for each configuration

7.5 Lift Analysis

The lift analysis of this aircraft will be combined with the high lift device considerations. Instead of having flaps as the traditional high lift device the SWAT team aircraft will utilize variable camber as well as a telescoping wing to create the increase in *cl*. These high lift devices will be utilized for landing, takeoff, and for better loiter times. The effects of the variable camber and telescoping can be seen in Table 7.2, which shows the *clmax* these devices are capable of reaching.

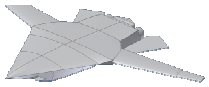

Table 7.2: Effect of sweep and camber on lift.

	NACA 23012		NACA 3012	
Sweep	***Cl alpha***	***Cl max***	***Cl max***	***Cl alpha***
20	0.1074	1.4529	1.5030	0.1038
20 w/ tel.	0.1105	1.4924	1.5475	0.1066
30	0.0960	1.3036	1.3445	0.0931
40	0.0815	1.1115	1.1414	0.0794
50	0.0691	0.9456	0.9681	0.0675
63	0.0441	0.6083	0.6172	0.0435

This data was calculated with equations used and verified in Brandt's textbook. These results are at, or better they what current fighters with complex flap systems are capable of. A typical fighter with advanced flaps can attain a usable lift coefficient of between 1.0 – 1.5 (Raymer, 12). The SWAT-5 concept with its sweep, telescoping, and camber can better the *cl*'s that flaps are able to produce.

7.6 RADAR Cross Section

One of the major design considerations for all future military aircraft will be the aircraft's RADAR signature. The quantity used to measure this quantity is an aircraft's RADAR Cross Section (RCS). An RCS can be presented in one of two scales: square meters or decibels. A modern fighter/attack aircraft, such as the F-15 generally has a RCS on the order or 25 m^2. More modern, low-observable, aircraft such as the F-22 have cross sections on the order of 0.5 m^2. This value is a key factor in determining how close an aircraft can approach a defended target without being detected and attacked.

Preliminary analysis of the RADAR Cross Section for the SWAT-5 Mako was conducted with the use of a MATLAB program named POFACETS. POFACETS is a publicly available physical optics based RCS program, developed by Elmo Garrido Jr., in which the subject aircraft is modeled by faceted surfaces (Garrido, 17.

Figure 7.11 depicts the results of this program for the fully swept configuration, with the front of the aircraft at a theta of 270°. The frontal RCS of approximately -2.5 decibels seen here

corresponds to a 0.56 m^2 cross section. Figure 7.12 shows the RCS for the un-swept configuration, which is almost identical to the swept configuration, though slightly higher throughout the spectrum. This number results from the fact that the basic layout of the SWAT-5 was designed with stealth considerations in mind. Low cross section values such as these will allow for even greater mission versatility.

Though this value looks acceptable at first glance, it must be noted that there are several important factors which this model does not take into account. This model does not account for the engine inlets, multiple reflections, or edge scattering, all of which will work to increase the cross section. However, this program also forces the user to assume a faceted shape, for which the number of facets is limited to 40, and assume a perfectly reflective body, all of which work to drive the RCS higher. Each of these, along with the knowledge that the developers of the program validated the results for a wide variety of models, leads to the conclusion that this may be a somewhat realistic preliminary estimate of the RCS.

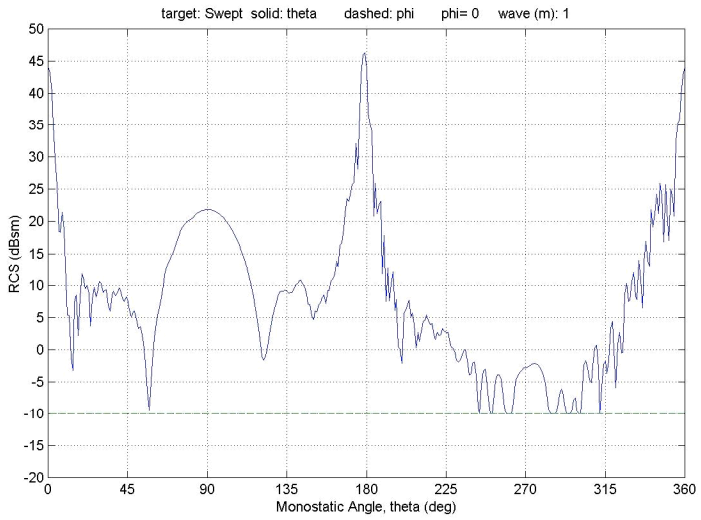

Figure 7.11: RADAR Cross Section of swept configuration

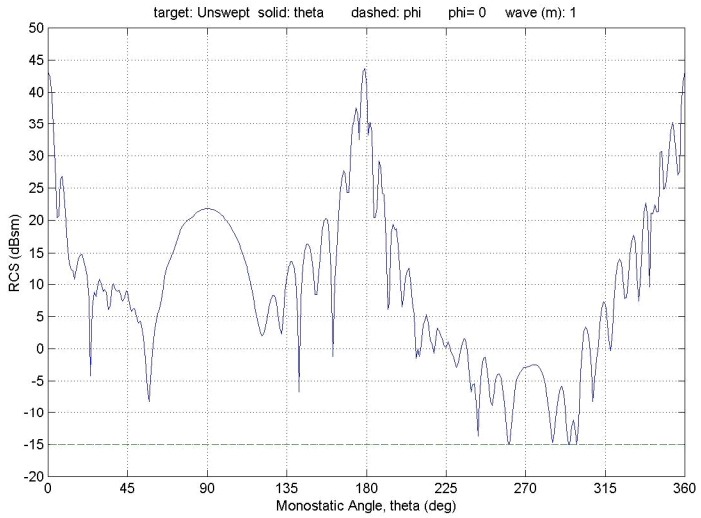

Figure 7.12: RADAR Cross Section of un-swept configuration

8 STABILITY AND CONTROL

8.1 Control Systems

As a morphing technology demonstration aircraft, the SWAT-5 incorporates several control morphing technologies in addition to the two mission morphing technologies of variable sweep and a telescoping wing section.

Longitudinal control is provided by the full flying horizontal tail and may be supplemented through the use of pitch thrust vectoring. A combination of controls can be created from the piezo-electric controls, variable camber, and adaptive torque tube to achieve the desired roll performance. If necessary, the horizontal tail and axisymmetric thrust vectoring systems are also available to provide lateral control power if needed. As the wings sweep back the effectiveness of the controls in the wings decreases, thus the horizontal tails will play an increasing roll in lateral control as the wings traverse through the sweep schedule. Directional control is available through the use of yaw thrust vectoring, the need for which is discussed later.

8.2 Static Stability

Unlike a conventional fixed wing aircraft, the static stability of the SWAT-5 will vary due to variation in the wing sweep angle and the telescoping wing section. Assessment of the static stability of the SWAT-5 was conducted through the use of TORNADO, a vortex lattice code developed by Tomas Melin. Aircraft models were developed to assess the effect of changing the wing sweep angle on the static stability of the aircraft in various sweep and telescoped configurations. Figure 8.1 shows an example of the models created for this purpose.

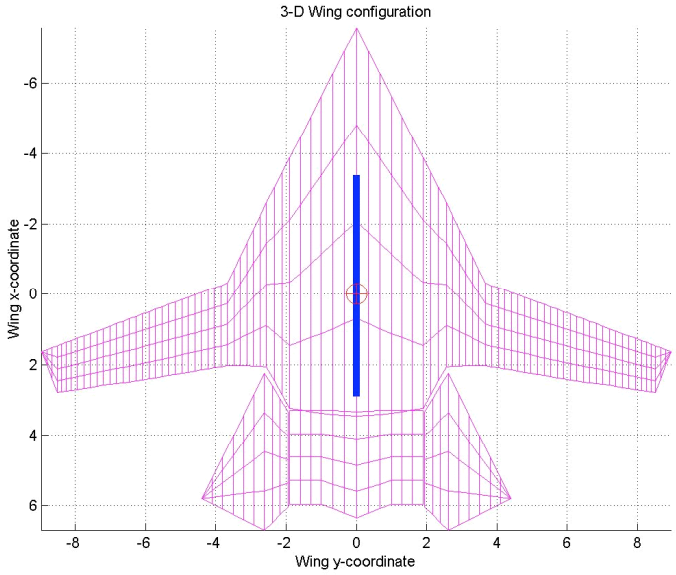

Figure 8.1: SWAT-5 baseline vortex lattice model from TORNADO.

To increase the accuracy of the stability results, a study was conducted to determine the effect of the number of panels in a model on the results provided by the code. As seen in Figure 8.2, after approximately 400 panels the variation of the neutral point location decreases significantly. The red circle in Figure 8.2 shows the current model configuration for the 20° sweep case with 504 panels. At the design point depicted the neutral point is varying approximately ±0.1" between tested points, which was determined to be a satisfactory uncertainty. It must also be noted that further increases in the number of panels increased the

required run-time for the code to unacceptable levels. The other models have the same basic layout with variations in the number of panels being caused by changes in the modeled wing area.

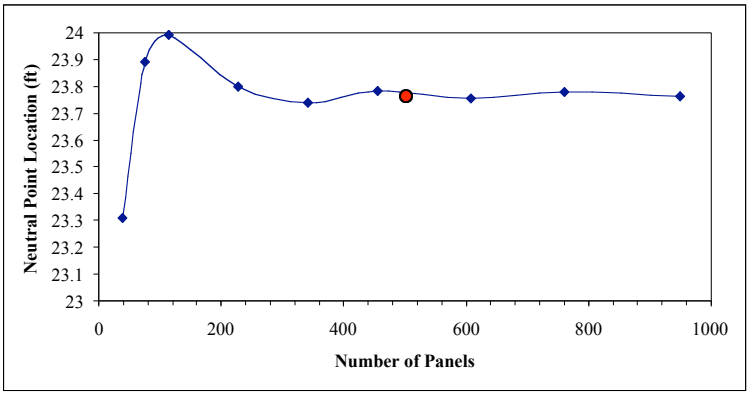

Figure 8.2: Shift in the calculated neutral point location due to the number of panels modeled. The red circle depicts the configuration for the model utilized for the stability analysis.

In terms of static stability, there are two major effects of variable sweep wings: neutral point variation, and center of gravity variation. Figure 8.3 depicts the movement of the aircraft's center of gravity as the wings are swept from the fully un-swept 19° position to the fully swept 63.4° position. The results of the center of gravity sweep are as expected in that the center of gravity continuously traverses aft as the wings are swept, and is slight more forward when the telescoping section is extended.

On the other hand, Figure 8.4 depicts the unexpected results of the neutral point variation. The results depict a small variation in neutral point location between sweep angles of 30° and 50° with large variations between 19° and 30° and between 50° and 63°. This same phenomenon is present with the telescoping sections extended; though the neutral point location is further aft for the telescoped position in general. It should be noted that the telescoping extension will only be used in the un-swept configuration for takeoff, landing, and cruise conditions.

The combination of the center of gravity and neutral point shifts result in the static margin variation found in Figure 8.5. These shifts result in the aircraft static margin varying between approximately 2% and 15% instability during normal configurations. For an aircraft of this type, a degree of instability of this magnitude is desired for increases in maneuverability and

decreases in trim drag. Further work still must be conducted to determine the effects of supersonic flight on the static margin.

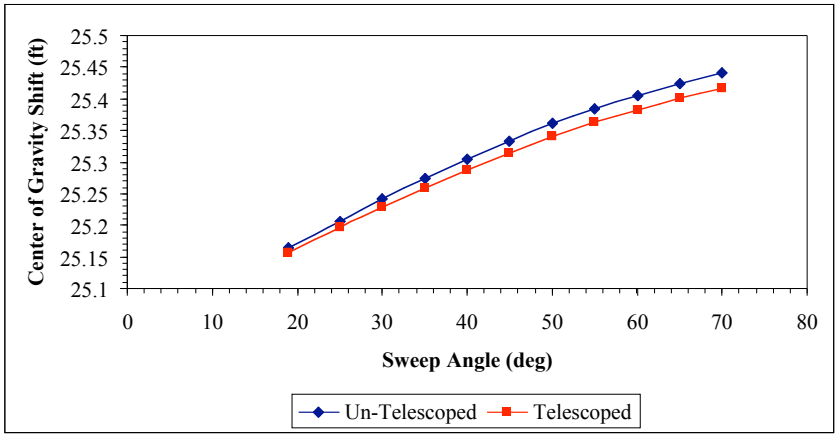

Figure 8.3: Center of gravity shift with sweep and span variation.

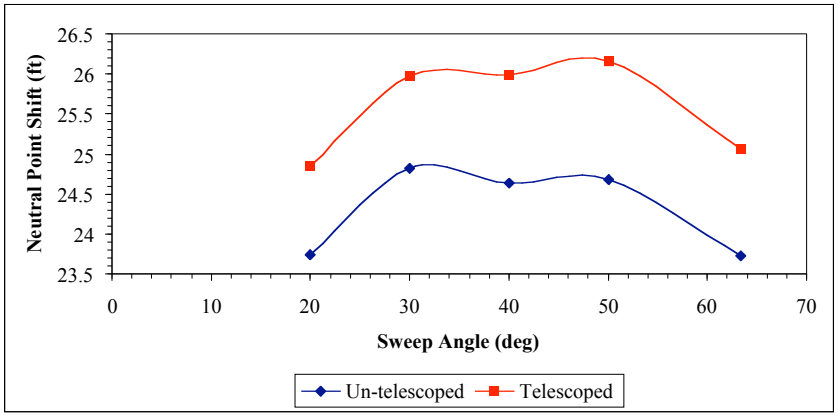

Figure 8.4: Neutral point shift with sweep and span variation.

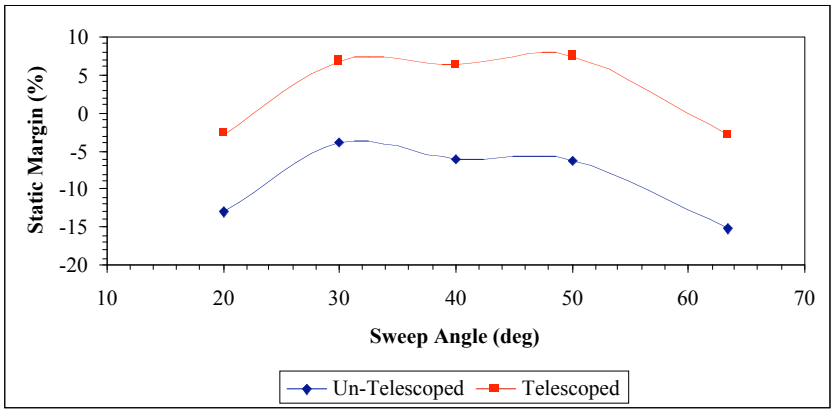

Figure 8.5: Static Margin shift with sweep and span variation.

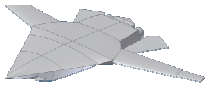

8.3 Stability Derivatives

Stability derivatives for the SWAT-5 were determined at takeoff conditions of M=0.3 for both the telescoped and un-telescoped configurations. Table 8.1 lists the relevant derivatives for the un-swept un-telescoped and un-swept telescoped configurations. The normal takeoff configuration will be the telescoped configuration. The only derivatives which could potentially cause problems are the C_Y and C_N derivatives which are low due to the fact that this aircraft does not have a vertical tail. These problems will be overcome through the use of thrust vectoring and a required stability augmentation system.

Table 8.1: SWAT-5 stability derivatives determined for the Un-Telescoped and Telescoped 20deg configuration as sea level takeoff conditions (M=0.3).

C_l Derivatives			C_m Derivatives			C_n Derivatives		
	Un 20	*Tel 20*		*Un 20*	*Tel 20*		*Un 20*	*Tel 20*
C	*0.0000*	0.0000	C	*0.1910*	-0.0019	C	*0.0000*	0.0000
C	*0.0318*	0.0308	C	*0.0000*	0.0000	C	*0.0192*	0.0149
C_{lp}	*-0.2784*	-0.3023	C_{mp}	*0.0000*	0.0000	C_{np}	*-0.0449*	-0.0537
C_{lq}	*0.0000*	0.0000	C_{mq}	*-0.9772*	-1.1772	C_{nq}	*0.0000*	0.0000
C_{lr}	*0.0322*	0.0352	C_{mr}	*0.0000*	0.0000	C_{nr}	*-0.0138*	-0.0087

C_L Derivatives			C_D Derivatives			C_Y Derivatives		
	Un 20	Tel 20		Un 20	Tel 20		Un 20	Tel 20
C	*3.5632*	3.8314	C	*0.1494*	0.1330	C	*0.0000*	0.0000
C	*0.0000*	0.0000	C	*0.0000*	0.0000	C	*-0.1269*	-0.1182
C_{Lp}	*0.0000*	0.0000	C_{Dp}	*0.0000*	0.0000	C_{Yp}	*-0.0477*	-0.0569
C_{Lq}	*2.8545*	3.3265	C_{Dq}	*0.1881*	0.1503	C_{Yq}	*0.0000*	0.0000
C_{Lr}	*0.0000*	0.0000	C_{Dr}	*0.0000*	0.0000	C_{Yr}	*-0.0640*	-0.0493

8.4 Engine Out Condition

The typical situation used to size a multi-engine aircraft's rudder is that of the engine out scenario. In this scenario the aircraft losses one engine on takeoff and must have sufficient rudder power to maintain zero sideslip on takeoff. In the case of the SWAT-5, which does not have a vertical surface, this situation was utilized to determine the effectiveness of the adaptive drag rudders. Assuming a sea level takeoff velocity of 335 ft/s (M=0.3) and a additional drag

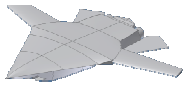

coefficient, ΔC_D=0.02 (Kapania, 18), based on the area behind the rudder, the adaptive drag rudder system was found to be grossly inadequate.

Without adding a vertical tail to the aircraft the only other option was yaw thrust vectoring. It was determined that a multi-axis axisymmetric thrust vectoring nozzle would be utilized. When the scenario was recalculated with the thrust vectoring it was found that the aircraft could meet the zero sideslip condition with a 12.7° thrust deflection, well short of the 20° maximum deflection generally characteristic of these systems.

9 PROPULSION SYSTEMS

A propulsion system was needed that could fulfill the mission requirements developed for this project. Namely, this was the ability of the aircraft to cruise at approximately Mach 0.9 yet be able to achieve supersonic speeds on the order of Mach 1.4 for short dashes. In this chapter, the propulsion system comparative study, thrust requirements, the selected propulsion system, and its characteristics and inlet geometry will be discussed.

9.1 Propulsion System Comparative Study

A comparative study of aircraft powerplants was conducted to come up with the best powerplant for the SWAT aircraft. The initial take-off gross weight (TOGW) estimate for the aircraft was 40,000 lbs. Through preliminary performance analysis, the team determined that the preliminary thrust to weight ratio (T/W) would be approximately 0.8. It might be noteworthy to notice that this is a little low compared to some supersonic bombers which are currently in the USAF inventory but this is mainly due to the fact that our design was made to cruise at transonic speeds. To obtain this thrust to weight ratio, a propulsion system was required that produced 16,000 lbs of thrust (Note that the concept utilizes two engines bringing the total thrust to 32,000 lb).

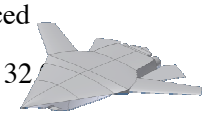

Eght engines were selected for the comparative study (Table 9.1). The Pratt & Whitney PW F100-220 and the General Electric F118-101, F110-100, F404/RM12, F404-400, F404-402, F404-102, and F404-F2J3 were the propulsion systems that were compared. The PW F100-220

was eliminated from selection due to the excessively high thrust and large Specific Fuel Consumption (SFC). It should be noted that this was the best contender from Pratt & Whitney even though the thrust was too high. The reason for this being that the alternate choices had dimensions that would not be acceptable for our project.

When looking through and coming up with the final choice, a great deal of emphasis was placed on Specific Fuel Consumption (SFC) and size. Surprisingly enough, the SPF varied from 0.66 to 1.98 among the different engine models which was strange since they all fell into the same size category. The dimensions also did not change a great deal especially among the General Electric engines. In fact, the last five engines listed in Table 9.1 have the same maximum diameter and engine length.

Table 9.1: Engine comparative study for various commercially available models. Data from www.geae.com and www.pratt-whitney.com

Model	Dry Weight (lb.)	Max Thrust (lb.)	SFC	Length (in.)	Max Diameter (in.)
PW F100-220	3,232	23,770	1.98	191	46.5
GE F118-101	3,150	17,000	0.66	110	47
GE F118-100	3,200	19,000	0.67	100.5	46.5
GE F404/RM12	2,325	18,100	1.78	154	35
GE F404-400	*2,195*	*16,000*	*1.85*	*154*	*35*
GE F404-102	2,282	17,700	1.74	154	35
GE F404-402	2,282	17,700	1.74	154	35
GE F404-F2J3	2,335	18,300	1.80	154	35

9.2 Thrust Requirements

The thrusts required at take-off, loiter, cruise, and dash were very important in the selection process. Thrust required (T_{REQ}) is a function of the density at a given altitude, velocity, wing area, and drag coefficient (assuming that it is flying at constant speed in which case the Thrust is equal to the Drag).

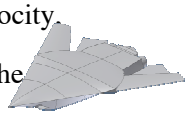

The thrust required divided by the number of engines is the total thrust required per engine in flight. The thrust required for the SWAT aircraft at the required altitudes and Mach numbers is tabulated in the Table 9.2.

Table 9.2: Thrust required from engines at given flight conditions

Condition	*Altitude (ft.)*	*Mach No.*	*Treq (lb.)*
Take-Off	0	0.25	20,000
Dash	40,000	1.42	32,000
Cruise	40,000	0.90	25,000
Loiter	30,000	0.40	20,000

9.3 Propulsion System Selected

Initially the General Electric F118-101 was chosen for the propulsion system of the aircraft. The main reason for this being that the SFC of 0.66 was significantly low compared to the others. Also, the thrust requirements based on max range and speed were met with a good margin by this engine.

However, it was decided by the group that thrust of 17,000 lb. was far in excess of what was really needed. Thus, it would be more useful to choose an engine model that had a higher SFC but gave the desired thrust of 16,000 lb. Additionally, this engine model was almost 1,000 lb. lighter. Consequently, the GE F404-400 was chosen.

Table 9.3: Base engine specifications. Data from www.geae.com

General Electric F404-400	
Physical Dimensions	
Fan/Compressor Stages	3/7
Low Pressure/ High Pressure Turbines	1/1
Maximum Diameter (Inches)	35.00
Length (Inches)	154.00
Dry Weight (lbs.)	2,195
Current Applications	F/A-18A/B
Power Specifications	
Maximum Specific Fuel Consumption	1.85
Maximum Thurst at Sea Level (lbs.)	16,000
Maximum Overall Pressure Ratio	26
Bypass Ratio	0.32

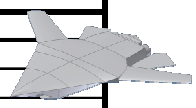

9.4 Inlet Geometry

The inlet system consists of a three-shock intake and a subsonic diffuser. The intake is double-wedge external compression. The double-wedge intake utilizes three shocks to slow the flow down from a maximum speed of Mach 1.4 to around Mach 0.5. The three shocks are composed of two oblique shocks (resulting from wedges placed in the inlet) and a normal shock. A diagram of the inlet is shown below:

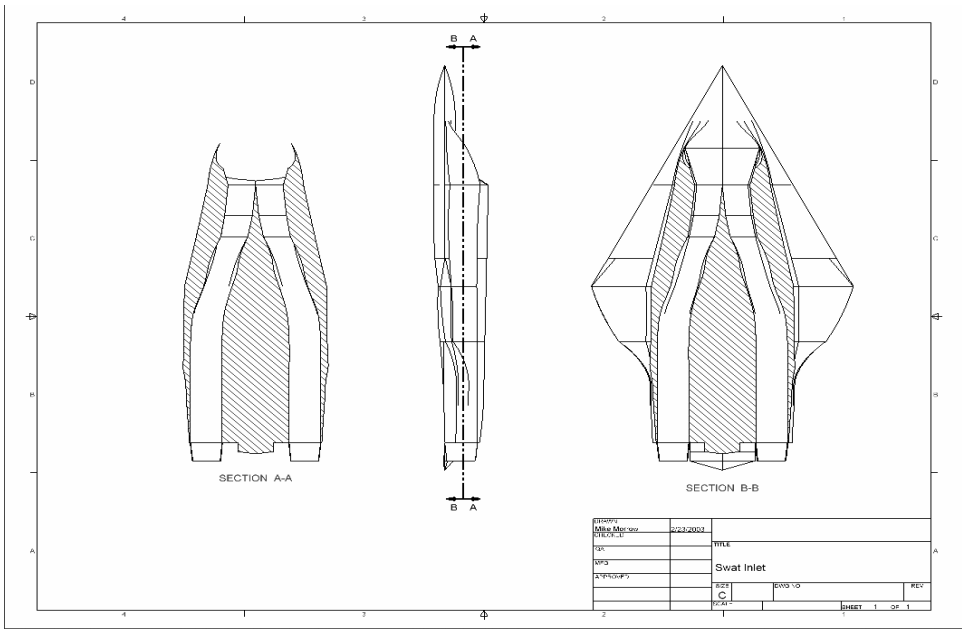

Figure 9.1: SWAT-5 S-Bend subsonic diffuser design.

The intake capture area was calculated using an equation found in Raymer. The capture area per engine is 11.95 ft^2. The diffuser (Figure 9.1) utilizes S-bend geometry to prevent the fan face from reflecting radar waves thus greatly contributing to the low Radar Cross-section (RCS) of the aircraft. In addition, radar absorbent material will be used in the inlet to further reduce the RCS, thus further contributing to the stealth characteristics of the aircraft. . Geometry of the diffuser further reduces the Mach number to 0.45 entering the fan face. A graph is shown in Figure 9.2that illustrates how the area varies in the diffuser from the inlet (labeled 0%) to the engine entrance (labeled 100%).

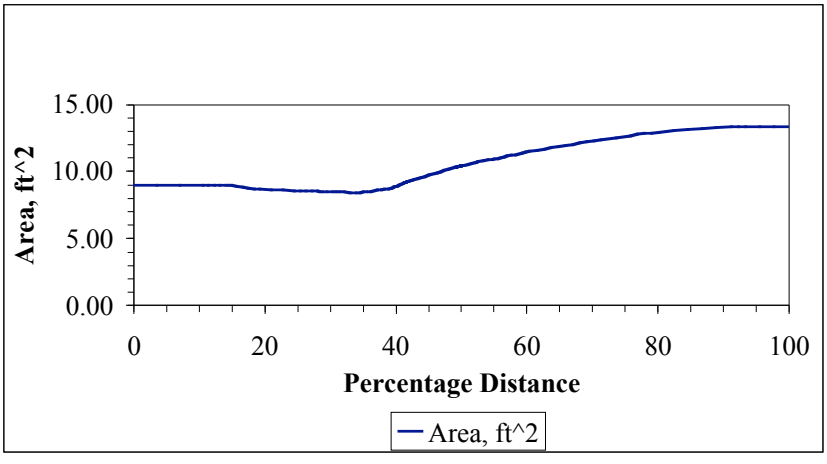

Figure 9.2: SWAT-5 inlet diffuser area variation.

10 STRUCTURES

10.1 V-n Diagram

The V-n diagram was constructed with a positive load factor limit of 9-gs and a negative load factor limit of 3-gs. These load factors were taken from limits of similar aircraft, values given in Raymer's text. Raymer's values for a fighter aircraft were between 6.5 and 9-gs for a positive load factor, and from -3 to 6-gs for the negative load factor (Raymer, 12). The diagram was constructed at the design cruise altitude of 40,000ft with the aircraft being in three different configurations. Configuration 1 (in light blue) is with the wings swept; this is the standard configuration for cruise. Configuration 2 (in dark blue) is with the wings un-swept, and configuration 3 (in red) is with the wings un-swept and telescoped. The equation to make the stall line is:

$$n_{\max} = C_{L\max} \frac{\frac{1}{2}\rho V^2}{\left(W/S\right)} \qquad (1.1)$$

where C_{Lmax} = 1.5, wing loading, W/S, depends on the configuration of the aircraft, and density, ρ, at 40,000ft (Megson, 19). This formula is used again but with the minimum C_L to calculate n_{min} in terms of velocity to give the negative stall line shown in Figure 10.1. Equation 1.1 can be used to find the maximum velocity by setting it equal to the load limit factor and solving for velocity. This, in addition to the dive velocity, gives the maneuver envelope shown in Figure 10.1.

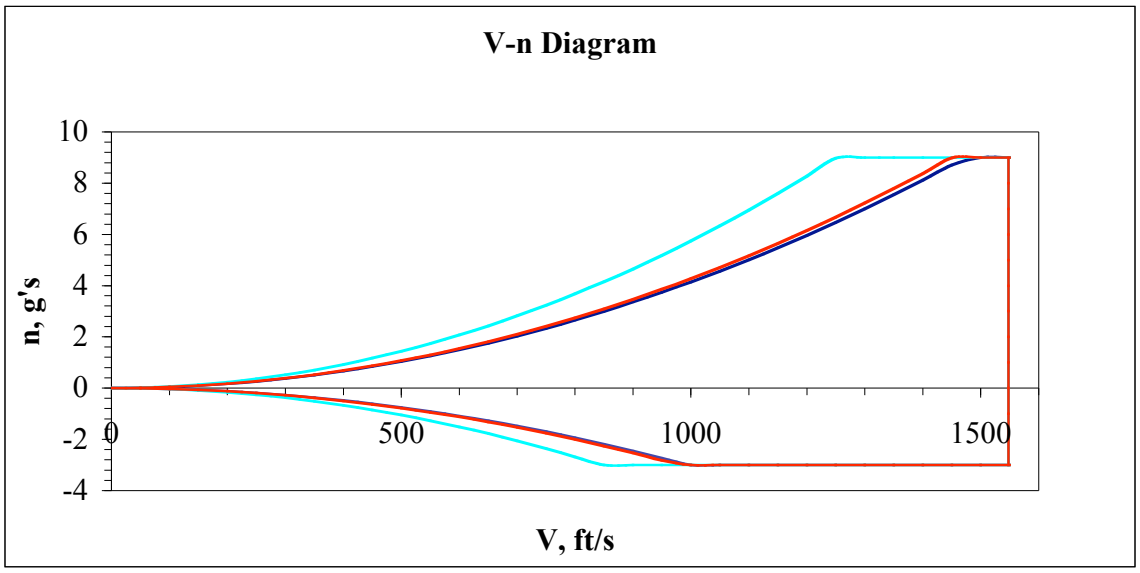

Figure 10.1: SWAT-5 V-n diagram for three different configurations. (Light Blue - Fully Swept, Dark Blue - Un-swept, Red - Un-swept and Telescoped)

10.2 Fuselage Structure

Transverse members in a body structure are known as bulkheads, and are designed to have specific duties within the fuselage. The fuselage structure is composed of multiple bulkheads placed along the length of the frame (Roskam, 20). Figure 10.2 shows the placement of each bulkhead down the length of the fuselage.

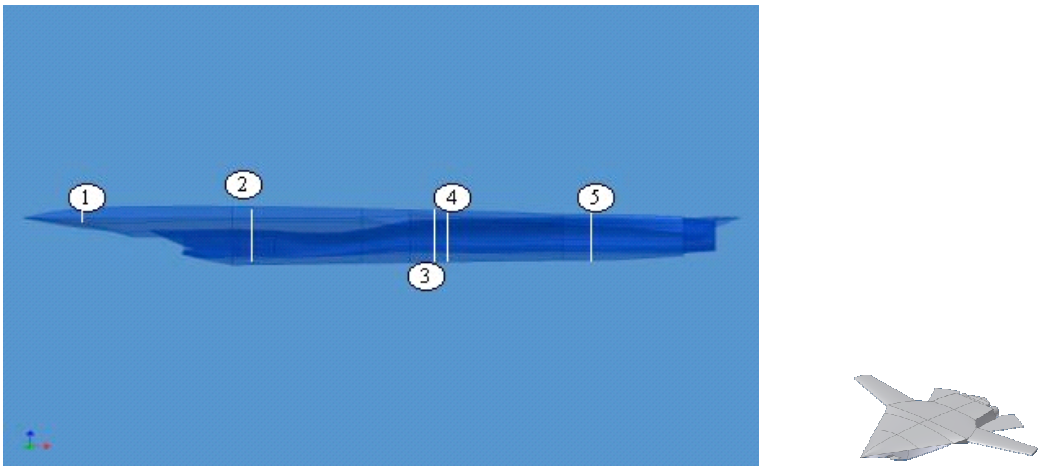

Figure 10.2: Bulkhead placement along fuselage.

In most cases bulkheads are more closely spaced near the front of the aircraft and the distance between each bulkhead gradually increases aft ward, this is not true for this aircraft. The

main use of a bulkhead is to maintain the cross-sectional shape of the fuselage. The bulkheads also distribute concentrated loads into the structure and redistribute stresses around structural discontinuities (Peery, 21). They also act with the skin to resist loads due to pressurization for non UCAV aircrafts. The first bulkhead is used to support internal systems placed in the nose of the aircraft. There are nose and main landing gear bulkheads, labeled in Figure 10.2 as #2 and #4. These two bulkheads are in place because of the high loads that are encountered during takeoff and especially landing. The aircraft also has a wing spar bulkhead #3, located at the pivot point of the swing wing. This bulkhead is one of the largest on the aircraft. The horizontal tail spar bulkhead, #5, is used to reallocate loads and stresses in this area.

10.3 Wing Structure

The wing structure is a complex one, constructed of ribs, spars, and torque tubes to create a desired twist distribution under any flight condition. Some added complexity to the structure is that the aircraft has variable camber and a variable sweep wing design. The layout of the win structure is shown in Figure 10.3.

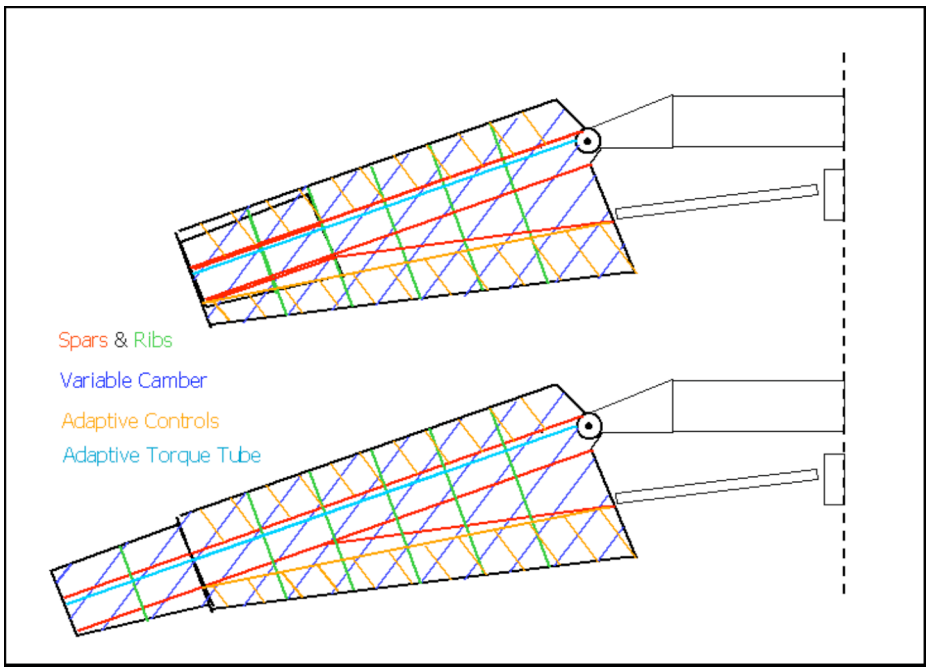

Figure 10.3: Internal wing structure

As illustrated in the Figure 10.3 the wing consists of a 5 rib and 3 spar system. The top two spars are aligned with the spars in the telescoping section of wing. This is done so that the wing can extend and retract along this axis. The spars are c-beams and the telescoping section will have smaller c-beams that fit in the larger main beams. A mechanical linkage is used to push and pull the wing extension when necessary. The ribs of the main wing and telescoping section are also aligned to minimize the effects of having a portion of the main wing structure gone when the wing is extended. With this design the wing will have only one hollow rib in the structure. The aircraft will experience smaller loads when the wings are extended (takeoff, landing, and loiter), the one hollow rib will not create enough structural instability for lengthy discussion.

The adaptive torque tube is located at the quarter cord of the wing. This design allows the wing twist to be controlled whenever necessary during flight. The torque tube will have an extending section that will continue out with the telescoping wing section. The variable camber and adaptive controls design will accomplished by using the Piezoelectric Fiber Composites. For the variable camber a layer of this will be applied across the entire wing including the telescoping portion. The adaptive control layer will be applied only on the main wing section and on only the trailing and leading edges. Application of this material will allow us to manipulate any section of the wing where the material is placed.

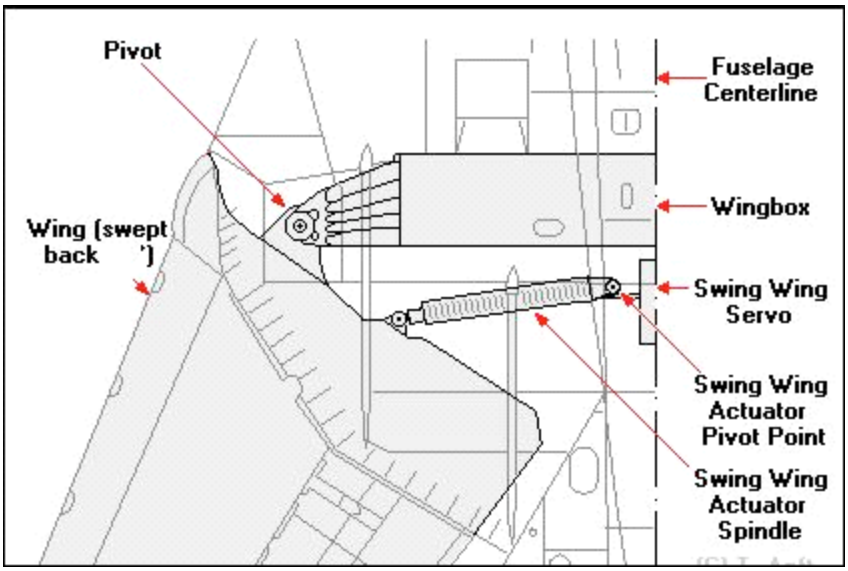

Figure 10.4: Variable sweep mechanism.

Picture from http://www.anft.net/f-14/f14-detail-gearnose.htm/

The variable sweep mechanism shown in Figure 10.4 illustrates the physical functionality of a variable sweep design. This mechanism is commonly used in aircrafts with variable sweep, such as the F-14. This design was used because it is commonly used and since it has been done we know that it works.

10.4 Landing Gear

Tricycle landing gear was chosen for this aircraft. This is the most frequently used landing gear configuration today. The main landing gear is located behind the center of gravity, while the nose landing gear is located in front of the center of gravity. Location of the nose landing gear was fairly tedious. The nose landing gear may not be placed in front of the inlet because it may warp the flow as it enters the inlet, also the wheel tends to send water and rocks inside the inlet (Raymer, 12). This is the reasoning for the placing the nose landing gear directly behind the split of the inlet. The main landing gear is used to support the majority of the aircraft weight at landing (roughly 90%). This was used in finding the correct placement aft of the center of gravity for the main landing gear.

Tire size was determined using Table 11.1 in Raymer. The nose tires are known to be anywhere from 60-100% of the size of the main landing gear. This aircraft has the nose gear 70% of the size of the main landing gear. This gives a main tire size of 30.65" in diameter, and 9.52" in width. The nose tire size is 21.45" in diameter, and 6.66" in width.

11 MATERIALS

The material selection was driven by the fact that the aircraft changes the configuration of its wing in several different ways, which would not be possible with conventional materials. This morphing puts constraints on the material selection because currently there are few products that can do what is needed for this aircraft. Particular sections of the aircraft did not require a selection process because there were no other competitors for the desired merchandise. Table 11.1 shows a variety of materials taken into consideration and Table 11.2 refers to a few important characteristics of each.

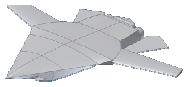

Table 11.1: SWAT-5 materials and their uses.

	Material	Usage
1	High strength unidirectional graphite/epoxy	Spar caps
2	High modulus ±45° graphite/epoxy	Skin (w/foam core), Shear web, Wing ribs
3	Aluminum 7075-T6	Bulkheads, Longerons
4	Stainless steel (AM-350)	Landing gear
5	Nickel (Hastelloy B)	Nozzles and ducting
6	Kevlar	Internal armor
7	PZT - EZ76 (Piezoelectric Fiber Composites)	Smart Controls
8	8552 Epoxy carbon Prepreg (Hexcel)	Fuselage

Table 11.2: Characteristics of materials from Table 15-2.

	Advantages	Disadvantages
1	High strength, low weight	High cost, low impact resistance, difficult to manufacture
2	High strength, low weight, low surface roughness, stealth characteristics	High cost, low impact resistance, difficult to manufacture
3	Low cost, ease of manufacture, good structural efficiency	Low strength, not weldable
4	Relatively low cost, high strength, corrosion resistance	High weight
5	Temperature resistance	Low structural resistance
6	High strength, low weight, high impact resistance	High cost, difficult to manufacture
7	Flexible and Light Weight	High cost
8	High strength, stiffness, and damage tolerance	

As shown from Table 11.2 the reason for picking a certain material is very evident. Strong, structurally effective materials were needed for the fuselage selection as well as for bulkheads. The materials utilzed encompass the characteristics necessary to successfully construct those particular parts of the aircraft. As for the controls of the aircraft only a flexible material would be sufficient because of the morphing technology. That is one reason why the PZT - EZ76 (Piezoelectric Fiber Composites) was selected, another reason is that it also incorporates the variable camber mechanisms within the material. With this material's flexibility and light weight this choice is the correct one. Many of the materials selected are high in cost; this is a reflection of the advanced ideas being used in this aircraft concept (Hexcel Corporation, 22).

A material not listed is a radar absorbent material (RAM), which will be used to help decrease the aircraft's RCS. RAM can be used by applying it on the aircraft as a thin coating on

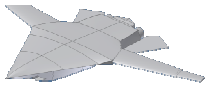

top the skin. The material will soon be in a more inexpensive paint form, this will allow it to be more widely used throughout the military. The RAM coatings are blip-resistant and help decrease reflected signals, which in turn increase the odds that it will be missed by enemy radar.

12 SYSTEMS AND PAYLOADS

12.1 Basic Layout

The layout of this aircraft is what is known as a blended wing body type layout. The weapons will be carried internally to reduce Radar Cross Section (RCS). Moreover, these weapons bays are conformal with the aircraft body and feature quick opening bay doors so that the weapons can be launched without the aircraft being illuminated by radar for too long.

12.2 Fire Control and Defensive Systems

The aircraft will have a variety of means of detecting threats and targets, both on the surface and in the air. The primary device is the Raytheon AN/APG–73 active array radar. The APG-73 is an all-weather, coherent, multimode, multi-wave form search-and-track sensor that utilizes programmable digital processors to provide the features and flexibility needed for both air-to-air and air-to-surface missions (Raytheon,23). This device is currently in service with the Navy's F/A-18 Super Hornet. It is mounted in the nose cone of the aircraft thereby allowing active scanning and ranging of airborne threats. Additionally, this radar array also provides the crew with a means of obtaining high-resolution radar maps of the ground (Raytheon, 23). In order to further reduce RCS, a selective bandpass radome will be placed in front of the radar thus only allowing the radiation from the AN/APG-73 to go through.

In addition this aircraft is also equipped with a Low Altitude Navigation and Targeting Infrared for Night (LANTIRN) targeting pod. This pod contains a laser range-finder/designator beam for precision-guided weapons, mostly "smart" bombs. Furthermore, it also incorporates a Forward Looking Infrared (FLIR) camera which allows the ground to be scanned (Raytheon, 23).

The LANTIRN and FLIR systems are both used with manned aircraft. However, the presence of these systems in a UAV will allow for greater capability for reconnaissance missions. The pod is mounted horizontally on the centerline of the aircraft behind the section where the cockpit is normally placed (behind the nose). Additionally, the FLIR pod is fully retractable serving to decrease both the drag and the radar signature of the aircraft. The LANTIRN navigation pod is mounted to the port side of the targeting pod and is also fully retractable.

12.3 Radar Cross Section (RCS)

In order to improve the RCS of the aircraft, no weapons will be housed externally. One item worth mentioning though is that the sidewinders are partially submerged on the outside since it was impossible store internally. Additionally, we have two optional hard points under the strakes to allow for external loads. Such configuration would only go into effect if the RCS was not a major issue for that particular mission i.e. close support or reconnaissance. This will also allow us to carry external drop tanks for the reconnaissance mission.

The engines are “buried” so that enemy radar cannot radiate straight down the inlet and illuminate the spinning fan blades, achieved through the use of an “S-shaped” inlet. Additionally, both the landing gear doors and the weapons bay doors are designed so that they can open and close in a very short period of time so that the aircraft is not illuminated for a significant period of time. Finally, the radome on the nose consists of single band-pass material allowing *only* the free travel of radar waves from the APG-73 radar system to go through but not the incoming threat radar frequency ranges.

12.4 Electrical System

Due to the large number of radar systems placed on this aircraft, there is a need for a large amount of electric power. To provide this, there are three separate electrical systems. The Auxiliary Power Unit (APU) is located in the tail and is primarily used to power the systems and avionics before and during takeoff. The two turbofan engines provide the main electric power to the aircraft using turbine generators, each of which can produce up to 90 kVa. The generator on

engine 1 (portside) is tied into the primary power harness while the generator of engine 2 (starboard) is tied into the secondary power harness (Raytheon, 23). Both of these are run separately through the aircraft to guarantee redundancy. The aircraft is also equipped with two sealed lead-acid batteries located behind the radars housed in the nose. In manned aircraft, these would serve to provide interior lighting, instrumentation, and power for APU start. However, since this aircraft is a UCAV, the batteries will be utilized in the event of an electrical failure for a short period of time.

12.5 Flight Controls

The aircraft is controlled by a derivative of the Fly-By-Wire system known as the Fly-By-Light system. This system functions similarly to the conventional Fly-By-Wire system, but has improved speed. Electro-Hydrostatic motors are used to operate all control surfaces and bays. These motors run off of the plane's electrical system (Raytheon, 23). The aircraft's motion is controlled by the control surfaces on it, including the "smart" surfaces. The presence of this type of a system offers a high degree of response accuracy in addition to removing the hydraulic controls used in conventional aircraft, which are heavy and often unreliable. Such technology however, does come at a cost. The main drawback to a Fly-By-Light control system is the relatively large power requirement. The two power generators would be more than enough to guarantee sufficient power.

12.6 Digital Flight Controller and Engine Control System

As mentioned above, the aircraft is controlled by means of a Fly-By-Light system. Since two systems are being used, a safeguard is provided in case one system malfunctions or stops working all together. When a control input is applied, the digital flight computer decides if the input is correct and then moves the appropriate surfaces to obtain the corresponding output. Such a mechanism creates similarity between this UCAV and manned aircraft since the computer keeps control inputs within required limits which could cause unnecessary stresses to structural components. Furthermore, the flight systems will have to be augmented for stability since the

aircraft is inherently unstable. Note that the flight controller would control the thrust vectoring nozzle as well.

12.7 Anti-Icing Equipment

Although many military aircraft do not have de-icing systems, the RFP states that this aircraft must perform in any and all possible flight conditions. Consequently, a de-icing system was integrated into the Mako system. This type of system consists of heating elements embedded in the leading edges of the wing and horizontal tail. This type of a system is commonly used on commercial aircraft.

12.8 Aircraft Lighting

The aircraft has minimal lighting due to the need for minimal visibility, radar or otherwise. Due to the fact that this aircraft can operate alone and is unmanned, there are no formation lights. Standard navigation lights are present, but can be switched off if there is a need to do so. These consist of a green light on the starboard wing and a red light on the port wing. Additionally, the nose landing gear has a landing light attached for taxiing and landing in poo light or fog.

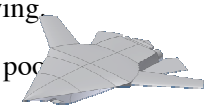

12.9 Weapons

The weapons specified by the RFP include AIM-9 Sidewinder missiles for close air-to-air combat as well as a variety of bombs ranging from 250 lb. to 1000 lb. These can be free fall or "dumb" bombs or guided "smart" bombs.

12.10 Bomb and Missile Bays

As mentioned earlier, no bombs will be housed externally so as to improve the Radar Cross Section of the aircraft for missions for which a low RCS is required. Since it is required that this aircraft perform its mission with minimal help from other assets, either escort aircraft or otherwise, it is equipped to carry air-to-air missiles in addition to its air-to-ground payload.

Due to flow interference at high speeds, munitions experience a force that tries to push them back into the aircraft when they are release, a problem that could cause serious problems in a mission. In order to rectify this problem, the bombs are mounted on lugs that are in turn attached to hydraulic pistons. When the signal is sent to employ a weapon, the bay doors open, the pistons extend, and a blast of inert gas generated by the on-board inert gas generation system (OBIGGS), pushed the weapon downwards from the aircraft with enough force so that the separation is sufficient to not cause the munitions to be pushed back into the bay (Raytheon, 23).

12.11 Defensive Systems

To effectively operate autonomously, this aircraft must be able to protect itself from enemy fire. This is cause for a number of defensive systems to be incorporated into the aircraft design. Most of these are located around the tail of the aircraft.

There is an AN/ALE-50 towed decoy developed by Raytheon. The AN/ALE-50 Towed Decoy System (TDS) is an Electronic Counter-measure (ECM) system designed for use on multiple U.S. Air Force, Navy and Marine Corps aircraft. It consists of three parts: a launch controller, launcher, and towed decoy (Raytheon, 23).

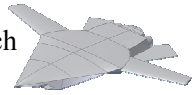

The launch controller contains the decoy control/monitor electronics and power supply and can be used on a wide variety of platforms without the need for modification. The launcher contains the decoy magazine and can be customized to fit a wide variety of aircraft. The decoy or “target” is packaged in a sealed canister and has a ten-year shelf life.

When deployed, the ALE-50's expendable aerial decoy is towed behind the host aircraft thereby protection the host aircraft against guided missiles by providing a more attractive radar target and luring RF missiles away from the aircraft and to the decoy. This stand-alone system requires no threat-specific software and communicates health and status to the host aircraft over a standard data bus.

In the event of an engagement, the aircraft is also equipped with an AN/ALQ-161A Integrated Electronic Warfare System (INEWS) and an Infrared Missile Warning System (IRMWS), both of which are also be obtained from Raytheon (Raytheon, 23). The purpose of these systems is to detect incoming missiles; both active radar targeted and infrared targeted thus alerting the computer system on the aircraft to release chaff and/or flares.

12.12 Internal Layout

Stealth design considerations necessitate that the SWAT-5 contain an internal weapons bay to hide the design ordinance from an enemy RADAR system. The weapons bay, seen in blue in Figure 12.0 is nominally 15 ft long, 4 ft high, and 6 ft wide and is situated such that the center gravity of the design ordinance load will coincide with the aircraft's center of gravity.

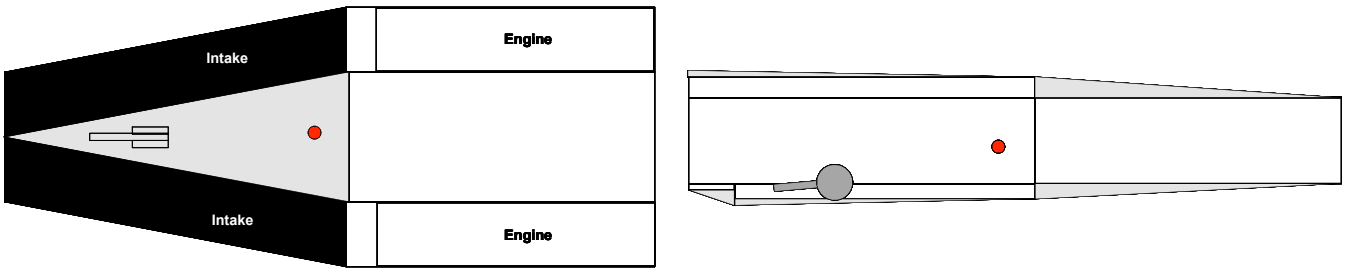

Figure 12.0: Internal Layout - Empty

The complexity of the SWAT-5 wing structure eliminates any possibilities of fuel storage within the wing. To accommodate the design 10,000 lbs. fuel requirement volumetric analysis was conducted. The SWAT-5 fuel system consists of nine fuel tanks which are collectively capable of holding 10,200 lbs. of JP-4 jet fuel. The locations of the main seven fuel tanks are seen in Figure 12.0 along with their respective center of gravities. Fuel tanks 8 and 9 are located just in front of the intakes between the intake and fuselage wall. In this configuration the SWAT-5's center of gravity only moves 0.42 ft between the fully fueled and empty configurations. This system will however require a fuel pumping system to maintain the desired center of gravity location as the fuel is used during the mission.

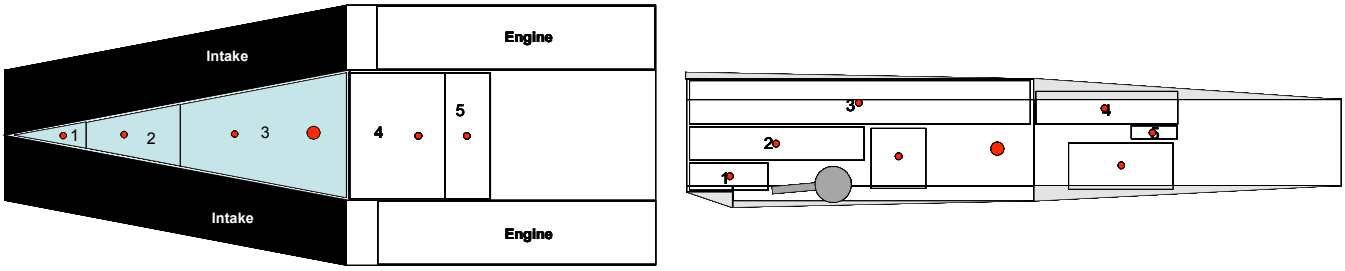

Figure 12.0: Internal Configuration - Fuel Layout

When in the fighter mission configuration the SWAT-5 will carry two AIM-120 AMRAAM missiles internally with two AIM-9X missiles carried partially submerged under the fuselage. This basic configuration is seen in Figure 12.0. Addition ordinance may be carried under-strake pylons if necessary.

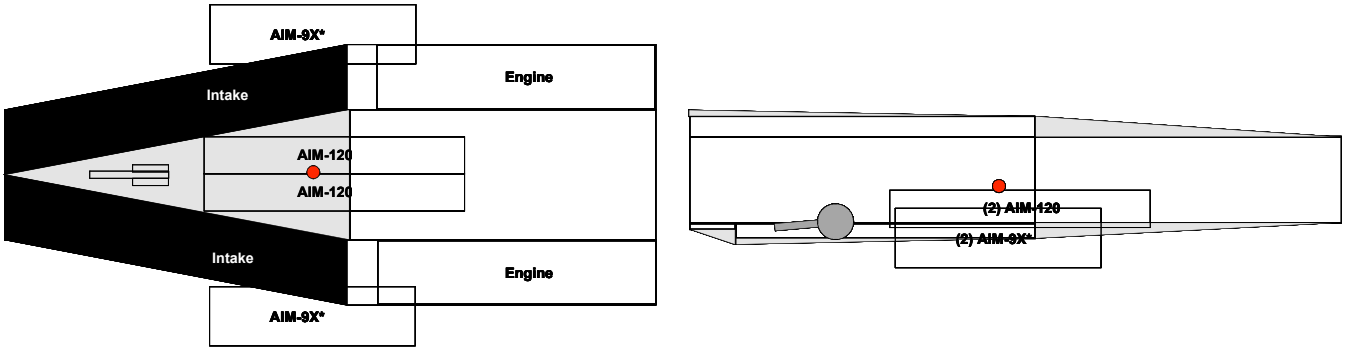

Figure 12.0: Internal Layout – Fighter Mission

The layout for the medium range strike mission consists of sixteen internally carried 250 lb. small diameter bombs, as seen in Figure 12.0, in addition to the base ordinance load. Again, additional ordinance can be carried on the under-strake pylons when stealth requirements are not as stringent.

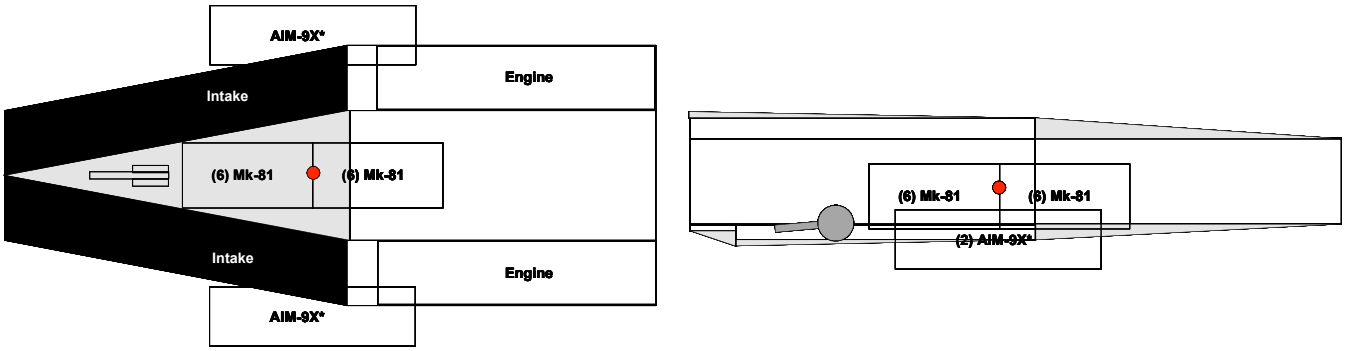

Figure 12.0: Internal Layout - Medium Range Strike Mission

The internal design load for the close air support mission includes six 250 lb. small diameter bombs and two AGM-65 air-to-ground missiles, as seen in Figure 12.0. Additional weapons or fuel can be carried under the strakes.

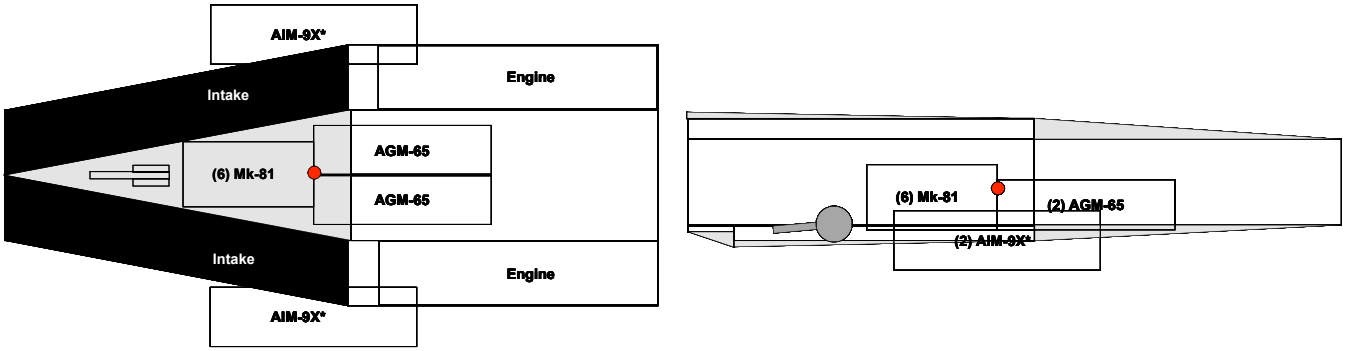

Figure 12.0: Internal Layout - Close Air Support Mission

The design requirements for the recon-quick strike mission profile require a total of 15,000 lbs. of fuel to complete the mission. To accommodate the extra fuel, empty space in the weapons bay is utilized for additional storage. The weapons bay for this mission contains six 250 lb. small diameter bombs and 3,100 lbs. of fuel, as seen in Figure 12.0. This fuel storage causes a center of gravity shift of 0.28 ft. Additionally, external 1,000 lb. fuel tanks will be carried under the strakes on each wing, bringing the total fuel load for this mission to 15,300 lbs.

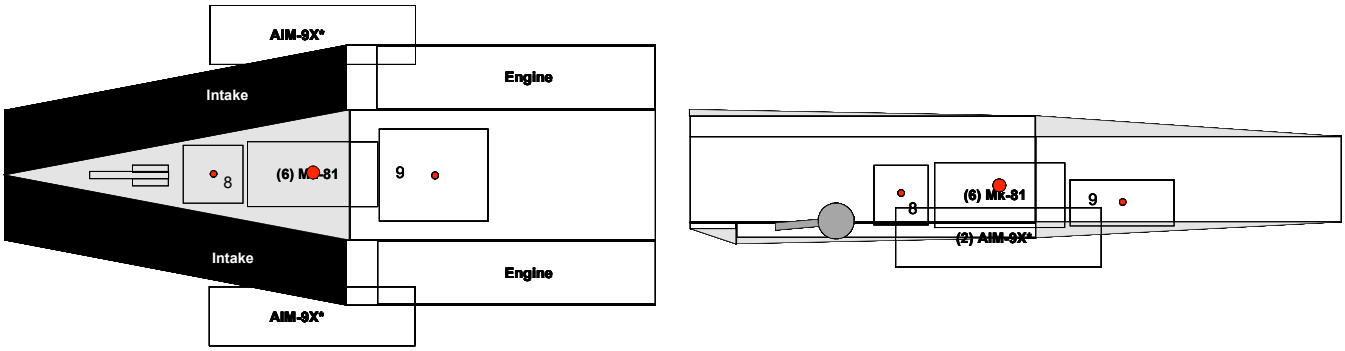

Figure 12.0: Internal Layout - Recon-Quick Strike Mission

13 WEIGHT ANALYSIS

13.1 Weight Composition

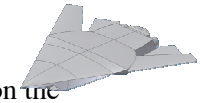

A study on the weight, center of gravity, and moments of inertia was completed on the SWAT-5. In order to determine a working empty weight, W_0, of the aircraft, Raymer's approximate weights methods (Raymer, 19) and Nicolai Aircraft Sizing Algorithm v0.9 (Mason, 15) were used. From these two methods, an initial take off gross weight estimate of 40,000 lbs and empty weight of 24,500 lbs were determined (Raymer, 19). These methods were verified using the F-14 Tomcat.

While the initial estimate was useful for decision-making, a more detailed examination was deemed necessary to study the aircraft's performance. To determine the components weights, a statistical group weights method- was used (Raymer, 12). This method is built upon sophisticated regression analysis of similar aircraft. Based on the missions and design of the SWAT-5, the fighter/attack model was used. Table 13.1 through Table 13.3 describe the composition of the weight groups. These tables are summarized in Table 13.4.

Table 13.1: Structural Weights

	Weight	Extended Telescope			Retracted Telescope			Swept		
		x_{cg}	y_{cg}	z_{cg}	x_{cg}	y_{cg}	z_{cg}	x_{cg}	y_{cg}	z_{cg}
	lbs	ft	ft	ft	ft	ft	ft	ft	ft	ft
Wing	1526	28.31	0.00	4.45	28.31	0.00	4.45	31.40	0.00	4.45
Telescope	167	31.72	0.00	4.43	29.76	0.00	4.43	37.63	0.00	4.43
Horizontal Tail	329.9	40.97	0.00	2.00	40.97	0.00	2.00	40.97	0.00	2.00
Fuselage	8678	24.28	0.00	3.27	24.28	0.00	3.27	24.28	0.00	3.27
Main Landing Gear	79.1	27.00	0.00	4.48	27.00	0.00	4.48	27.00	0.00	4.48
Nose Landing Gear	25.0	24.60	0.00	2.20	24.60	0.00	2.20	24.60	0.00	2.20
Total	10805.1	25.49	0.00	3.42	25.46	0.00	3.42	26.02	0.00	3.42

Table 13.2: Propulsive Weights

	Weight	x_{cg}	y_{cg}	z_{cg}
	lbs	ft	ft	ft
Engines	4564	28.17	0.00	2.50
Engine Mounts	131.1	28.00	0.00	2.50
Engine Section	69.1	28.00	0.00	2.50
Air Induction System	1150	20.00	0.00	2.00
Engine Cooling	341	28.00	0.00	2.50
Oil Cooling	77	28.00	0.00	2.50
Engine Controls	30	20.00	0.00	3.00
Starter (pneumatic)	70	28.00	0.00	2.50
Total	6431.3	26.65	0.00	2.41

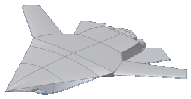

Table 13.3: System Weights

	Weight	x_{cg}	y_{cg}	z_{cg}
	lbs	ft	ft	ft
Fuel System and Tanks	1169	17.00	0.00	3.00
Flight Controls	532	10.00	0.00	3.50
Hydraulics	193	26.00	0.00	4.00
electrical	758	28.00	0.00	3.00
avionics	1333	18.00	0.00	3.50
air conditioning and anti-ice	231	25.00	0.00	2.00
handling gear	12	26.00	0.00	2.00
Total	4226	19.28	0.00	3.21

Table 13.4: Weight Summary

	Weight	Extended Telescope			Retracted Telescope			Swept		
		x_{cg}	y_{cg}	z_{cg}	x_{cg}	y_{cg}	z_{cg}	x_{cg}	y_{cg}	z_{cg}
	lbs	ft	ft	ft	ft	ft	ft	ft	ft	ft
Structural	10805.1	25.49	0.00	3.42	25.46	0.00	3.42	26.02	0.00	3.42
Propulsions	6431.3	26.65	0.00	2.41	26.65	0.00	2.41	26.65	0.00	2.41
Systems	4226	19.28	0.00	3.21	19.28	0.00	3.21	19.28	0.00	3.21
Ordinance	5500	26.00	0.00	3.00	26.00	0.00	3.00	26.00	0.00	3.00
Fuel	10230.19	23.36	0.00	3.92	23.36	0.00	3.92	23.36	0.00	3.92
Recon Fuel - Internal	3103.83	26.27	0.00	1.99	26.27	0.00	1.99	26.27	0.00	1.99
W0	21462.8	24.62	0.00	3.08	24.60	0.00	3.08	24.88	0.00	3.08
TOGW	37193.0	24.48	0.00	3.30	24.47	0.00	3.30	24.63	0.00	3.30
TOGW - Recon	40296.8	24.61	0.00	3.20	24.61	0.00	3.20	24.76	0.00	3.20

13.2 Center of Gravity

In order to determine the center of gravity of the different configurations, the individual centers of gravity for the components were determined. By summing the moments caused by the components about the nose, the configuration's center of gravity could be determined by dividing by the combined weight of the components.

13.3 Moment of Inertia

In order to determine the mass moment of inertia of the entire aircraft, the individual mass moments of inertia of the components were determined. These were computed with the origin at the center of gravity of the individual part, and the axes were aligned with the axes of the aircraft. This setup allowed the mass moment of inertia to be shift via the parallel-axis theore

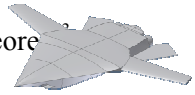

The compiled values can be seen in Table 13.4.

14 COST

The cost of the SWAT-5 Mako was determined using a method suited for prototype and flight demonstrators (Raymer, 12). This method estimated 90 work hours per pound of wing, and 50 work hours per pound of fuselage. This value was increased to 150 work hours per pound, based on the complexity of the airfoil used. A summary of the costs for the SWAT-5 Mako are listed in Table 14.1.

Table 14.1: SWAT-5 cost estimate

	Weight	Time	Cost
	lbs	hrs	10^6
Wing	1526	228855	19.682
Telescope	167	25044	2.154
Horizontal Tail	329.9	29689.9	2.553
Fuselage	8678	433920	37.317
Propulsion	-	-	3.000
Avionics	-	-	2.000
Total	10805.1	717509.2	66.706

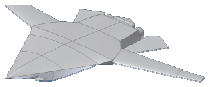

15 REFERENCES

1. Kral, Linda. Active Flow Control Technology, ASME Fluids Engineering Division Technical Brief.

2. McGowan, Anna. "Like a Bird's Wing," SAIC Information Services. 2002 avail: http://www.aero-space.nasa.gov/curevent/news/vol2_iss6/bird.htm

3. Simpson, J.O. Innovative Materials for Aircraft Morphing. Materials Division NASA Langely Research Center.

4. Uchino, K., "Designing with Piezoelectric Devices," Partial Contribution to Designing with Engineering Ceramics, Amer. Ceram. Soc., PA (2002). [in press]

5. Ashley, Steven. "Magnetostrictive Actuators." American Society of Mechanical Engineers. 1998 avail: http://www.memagazine.org/backissues/june98/features/magnet/magnet.html

6. Gibbs, Gary P., Cabell, Randolph H. "Active Control of Turbulent Boundary Layer Induced Sound Radiation from Multiple Aircraft Panels", AIAA-2002-2496

7. Pinkerton, Jennifer L., McGowan Anna-Maria R., Moses, Robert W., Scott, Robert C., Heeg, Jennifer "Controlled Aeroelastic Response and Airfoil Shaping using Adaptive Materials and Integrated Systems", NASA Langley Research Center February February 26, 1996

8. Erickson, Gary E., Murri Daniel G., "Wind Tunnel Investigations of Forebody Strakes for Yaw Control on F/A-18 Model at Subsonic and Transonic Speeds"

9. Montoya, L. C., Flechner, S. G., Jacobs P. F., "Effect of an Alternate Winglet on the Pressure and Spanwise Load Distributions of a First Generation Jet Transport Wing" NASA-TM-78786

10. http://www.geversaircraft.com/

11. Asker, James R. ed. "Small And Supersonic." *Aviation Week & Space Technology*. 12 August 2002. Page 23.

12. Raymer, Daniel P., *Aircraft Design: A Conceptual Approach 3rd Edition*. American Institute of Aeronautics and Astronautics: Reston, Virginia. 1999

13. Morrow, Michael. "Virginia Tech Aircraft Design Software Series: Aircraft Performance". Virginia Tech: Blacksburg, VA. 2002.

14. Robert W. Kress, "Variable Sweep Wing Design," in Evolution of Aircraft Wing Design, March 18-19, 1980, Dayton, Ohio, AIAA Paper 80-3043, 1980.

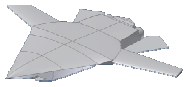

15. Mason, W.H. Nicolai Aircraft Sizing Algorithm v0.9. Virginia Tech Aerospace Software Series: Blacksburg, Virginia.

16. Brandt, Steven A., Stiles, Randall J. Bertin, John J., Whitford, Ray. Introduction to Aeronautics: A Design Perspective. American Institute of Aeronautics and Astronautics: Reston, Virginia. 1997

17. Garrido, Elmo E. Jr.. POFACETS (Matlab Code), September 2000

18. Kapania, R., Natarajan, A., Inman, D., "Aeroelastic Analysis of Adaptable Bumps Used as Drag Rudders," AIAA-02-0707

19. Megson, T.H.G., Aircraft Structures for Engineering Students, John Wiley & Sons Inc. New York, 1999

20. Roskam, Jan, Airplane Design Part III, DARcorporation Lawerence, Kansas, 2002

21. Peery, David J., Aircraft Structures, McGraw-Hill Book Company New York, 1982

22. Hexcel Coporation, www.hexcelcomposites.com; Pleasonton, CA

23. www.raytheon.com